

RESEARCH

Open Access



Comparative transcriptome and coexpression network analysis revealed the regulatory mechanism of *Astragalus cicer* L. in response to salt stress

Yujuan Zhang^{1,2}, Wenke Dong^{1,2*}, Huiling Ma^{1,2}, Chunxu Zhao^{1,2}, Fuqin Ma^{1,2}, Yan Wang^{1,2}, Xiaolin Zheng^{1,2} and Minhui Jin^{1,2}

Abstract

Background *Astragalus cicer* L. is a perennial rhizomatous legume forage known for its quality, high biomass yield, and strong tolerance to saline-alkaline soils. Soil salinization is a widespread environmental pressure. To use *A. cicer* L. more scientifically and environmentally in agriculture and ecosystems, it is highly important to study the molecular response mechanism of *A. cicer* L. to salt stress.

Results In this study, we used RNA-seq technology and weighted gene coexpression network analysis (WGCNA) were performed. The results showed 4 key modules were closely related to the physiological response of *A. cicer* L. to salt stress. The differentially expressed genes (DEGs) of key modules were mapped into the KEGG database, and found that the most abundant pathways were the plant hormone signal transduction pathway and carbon metabolism pathway. The potential regulatory networks of the cytokinin signal transduction pathway, the ethylene signal transduction pathway, and carbon metabolism related pathways were constructed according to the expression pathways of the DEGs. Seven hub genes in the key modules were selected and distributed among these pathways. They may involved in the positive regulation of cytokinin signaling and carbon metabolism in plant leaves, but limited the positive expression of ethylene signaling. Thus endowing the plant with salt tolerance in the early stage of salt stress.

Conclusions Based on the phenotypic and physiological responses of *A. cicer* L. to salt stress, this study constructed the gene coexpression network of potential regulation to salt stress in key modules, which provided a new reference for exploring the response mechanism of legumes to abiotic stress.

Keywords Salt stress, *Astragalus cicer* L., Physiological and biochemical, RNA-seq, WGCNA

Background

Soil salinization is a widespread environmental stress in natural and agricultural ecosystems. The total area of saline-affected soils is well over 900 million hectares worldwide and continues to increase [1, 2]. The effects of salt stress on plants mainly originate from osmotic stress and ion toxicity [3, 4]. Excessive soluble salts in soil reduce the water potential of the soil around the plant

*Correspondence:

Wenke Dong
dongwk@gsau.edu.cn

¹ College of Grassland Science, Gansu Agricultural University, Lanzhou 730070, China

² Key Laboratory of Grassland Ecosystem (Gansu Agricultural University), Ministry of Education, Lanzhou 730070, China



© The Author(s) 2024. **Open Access** This article is licensed under a Creative Commons Attribution-NonCommercial-NoDerivatives 4.0 International License, which permits any non-commercial use, sharing, distribution and reproduction in any medium or format, as long as you give appropriate credit to the original author(s) and the source, provide a link to the Creative Commons licence, and indicate if you modified the licensed material. You do not have permission under this licence to share adapted material derived from this article or parts of it. The images or other third party material in this article are included in the article's Creative Commons licence, unless indicated otherwise in a credit line to the material. If material is not included in the article's Creative Commons licence and your intended use is not permitted by statutory regulation or exceeds the permitted use, you will need to obtain permission directly from the copyright holder. To view a copy of this licence, visit <http://creativecommons.org/licenses/by-nc-nd/4.0/>.

root system, causing plants to have higher water potential than that of their growing soil. Therefore, limiting their absorption and utilization of water and leading to water deficiency in the plants' cells [5]. A decrease in plant cell water induces stomatal closure which affects CO₂ fixation, resulting in reduced efficiency of photosynthesis and increased accumulation of reactive oxygen species (ROS). Therefore, photosynthesis and ROS changes affect the fixation and assimilation of carbohydrates by altering enzyme activity and plant hormone levels and causing disturbances in other metabolic systems [6]. Plants maintain the balance of K⁺ and Na⁺ in the cytoplasm through K⁺/Na⁺ transport proteins and H⁺ pumps. When salt stress occurs, the absorption rate of K⁺ in plant cells is inhibited by excessive Na⁺ ions in the soil, which affects the activity of K⁺ dependent enzymes in the cytoplasm [7]. Under high salt stress, the influx of Na⁺ through non-selective cation channels (NSCCs) and cation transporter proteins may also inhibit the inward flow of K⁺ and Ca²⁺. The high concentrations of Na⁺ may cause depolarization of the cytoplasmic membrane, leading to the efflux of K⁺ and Ca²⁺ and thereby affecting the signal transduction process of the plant and leading to nutrient element deficiency [8]. Additionally, the absorption and accumulation of Cl⁻ also antagonize NO₃⁻ uptake, resulting in a lack of essential nitrogen [9].

Through long-term evolution, plants have also developed a series of response mechanisms to abiotic stress such as altering the ratio of osmotic substances [5], activating antioxidant enzyme systems, redistributing ions [10], and accumulating carbohydrates [11]. Furthermore, salt stress also triggers plant stress responses and gene activation, osmotic proteins, water channel proteins, genes related to signal transduction, energy metabolism, and hormone signaling [12]. In the salt overly sensitive pathway (SOS) in response to salt stress, abnormally changing intracellular Ca²⁺ signals are sensed by SOS3, which activates SOS2 kinase [13]. After SOS2 is activated, it further phosphorylates SOS1 to mediate Na⁺ efflux, enabling plants to achieve salt tolerance [13]. Genes related to the endogenous protein PIP in the plasma membrane enhance photosynthesis by increasing the conductivity rate of chloroplastic CO₂ in the phloem system [14]. And the protein also increases the sucrose transport rate, root hydraulic conductivity, water use efficiency, and accumulation of hydrophilic metabolites to alleviate salt stress [14]. The abscisic acid (ABA) signaling pathway promotes salt secretion in the leaf salt gland by inducing the expression of downstream *MYB* transcription factors. The accumulation of ABA indirectly enhances leaf salt tolerance by affecting deterrent proteins, increasing the content of jasmonic acid (JA), contributing to the production of a small amount of ethylene

(ETH) and ROS, and enhancing the activity of plant antioxidant enzymes [15].

Astragalus cicer L. is a perennial herbaceous plant belonging to the genus *Astragalus* in the family Leguminosae. It has high-quality, high-yield, high-nutritional value, amino acid-rich and widely adapted perennial rhizomatous legume forage [16, 17]. Its developed and sinuous roots and stems allow it to grow not only in rough soils but also in saline, drought, and acidic soils. It also has nodules, which improve soil fertility, nitrogen fixation, and other soil properties. Thus, *A. cicer* L. is a good grass species for soil and water conservation and the establishment of long-term artificial grasslands [17], and suitable for planting in sandy wasteland, low yield field and saline alkali land. The transcriptomic analysis is currently one of the most widely used high-throughput sequencing analysis techniques and is used to find DEGs, marker genes, and synergistic change genes by comparing different transcripts. Additionally, transcriptomic analysis results are functionally annotated and visually displayed [18]. Weighted gene coexpression network analysis (WGCNA) is a systems biology method that analyzes the gene expression patterns of multiple samples. This method aims to identify expression modules associated with specific traits or phenotypes and is an effective approach for studying gene regulatory networks [19]. A comprehensive analysis of these two methods can aid in more accurately understanding the dynamic response process of plants to external environmental changes and determining the key regulatory mechanisms of plant resistance [20].

In this study, based on evaluating the phenotypic and physiological responses of *A. cicer* L. to salt stress. We used Illumina NovaSeq™ 6000 to perform transcriptomic sequencing analysis of *A. cicer* L. under salt stress at different times and used WGCNA to explore the response of *A. cicer* L. to salt treatment in key modules and constructed potential regulatory networks of the cytokinin signal transduction pathway, ethylene signal transduction pathway, and carbon metabolism-related pathways, and the potential regulatory relationships between the hub genes and salt stress in each subnetwork were analyzed. This investigation provided a new reference for exploring the response mechanism of leguminous plants in response to abiotic stress.

Results

Effect of salt stress treatment on the physiological characteristics of *A. cicer* L.

We found that the phenotypic traits of the *A. cicer* L. leaves at 1–7 d after treatment with 150 mmol·L⁻¹ NaCl stress were similar to those at 0 d (CK). Few old leaves began to curl slightly at 7 d, a few new leaves turned

yellow at 14 d and some leaves began to curl, and nearly half of the leaves curled and accompanied by the plant lateral drooping and wilting at 21 d (Fig. 1). The relative electrical conductivity (REC) and malondialdehyde (MDA) content indicate the severity of oxidative damage in plants under salt stress [21]. The results of this study showed that with increasing stress duration, the REC and MDA content of the *A. cicer* L. seedlings showed a pattern of initially increasing, then decreasing, followed by another increase. Both REC and MDA decreased to their lowest levels at 7 d of stress. At this time, the REC did not significantly differ between 7 and 5 d. In contrast, the MDA content was significantly lower than that in the other time points ($P < 0.05$) (Fig. 2A and B).

ROS mainly exists in the form of $O_2^{\cdot-}$ and H_2O_2 , which can act as signaling molecules to induce plant resistance responses. However, their increase can also cause damage to plant somatic cells and other important physiological process systems [22]. The results showed that the changes in $O_2^{\cdot-}$ and H_2O_2 content in the seedlings varied with different stress durations. At 1 d of NaCl stress, $O_2^{\cdot-}$ increased compared to that in the CK group (0 d), then slowly decreased to the minimum value at 5 d, and then slowly increased again and was significantly greater than that in the CK group at 14 d and 21 d ($P < 0.05$) (Fig. 2C). However, the H_2O_2 content was significantly lower than that in the CK group at 1 d of NaCl stress ($P < 0.05$) and then increased to the maximum value at 7 d before slowly decreasing (Fig. 2D).

The antioxidant system of plants is composed of superoxide dismutase (SOD, EC 1.15.1.1), peroxidase (POD, EC 1.11.1.7), and catalase (CAT, EC 1.11.1.6), which together control the accumulation of ROS and regulate plant tolerance to environmental pressure [23]. The results of this study revealed that the activity trends of the three antioxidant enzymes were different. Specifically, SOD activity was significantly greater in the salt stress treatment group than in the CK group at 1 d and 3 d of NaCl stress ($P < 0.05$) and then slowly decreased to 50.56% of that in the CK group at 21 d (Fig. 2E). Although

POD activity increased from 1 to 7 d under salt stress, there was no significant difference between adjacent treatment times; however, POD activity significantly increased from 14 d and was 2.83 times greater than that in the CK group at 21 d (Fig. 2F). The CAT activity of the plants in the salt stress treatment group was greater than that in the CK group from 1 to 14 d and reached its maximum at 7 d but lower than that in the CK group at 21 d, but the difference was not significant (Fig. 2G).

Proline (Pro), soluble sugars (SS), and soluble proteins (SP) are three common organic osmoregulatory substances in plant cells; under salt stress, Pro is a key substance used by plants to regulate osmotic balance; and SS and SP are crucial for the water retention ability of plant cells [24, 25]. The Pro and SS contents of *A. cicer* L. continued to increase with increasing salt stress duration, and the contents of both were greater than those in the CK after NaCl stress treatment. The Pro and SS contents were 4.19 times and 1.84 times greater, respectively than those in the CK at 21 d (Fig. 2H and I); the SP content showed an overall upward trend in the early stage of NaCl stress, reached its maximum value at 5 d, which was 1.30 times that of the CK, and then gradually decreased until reaching its minimum value at 21 d, which was 84.17% of that of the CK (Fig. 2J).

Statistics of sequencing results

To comprehensively understand the transcriptome and gene expression profile of *A. cicer* L. under salt stress at different times, the Illumina HiSeq 6000 platform was used to sequence 15 cDNA samples extracted from the leaves of *A. cicer* L.. A total of 605,219,946 raw reads were obtained from 15 samples. After removing the splices, poly-A/T sequences, and low-quality sequencing reads, a total of 576,956,974 valid reads were obtained which were 84.9 G (Gbase, Gb) in size (Additional file 1: Table S1). There were more than 36 million raw reads and valid reads generated from each sample, with more than 90% valid bases above 5.0 G (Gbase, Gb), more than 95.00% valid bases, more than 90.00% Q30, and between 42.25%



Fig. 1 Phenotypes of *A. cicer* L. under salt stress at different times

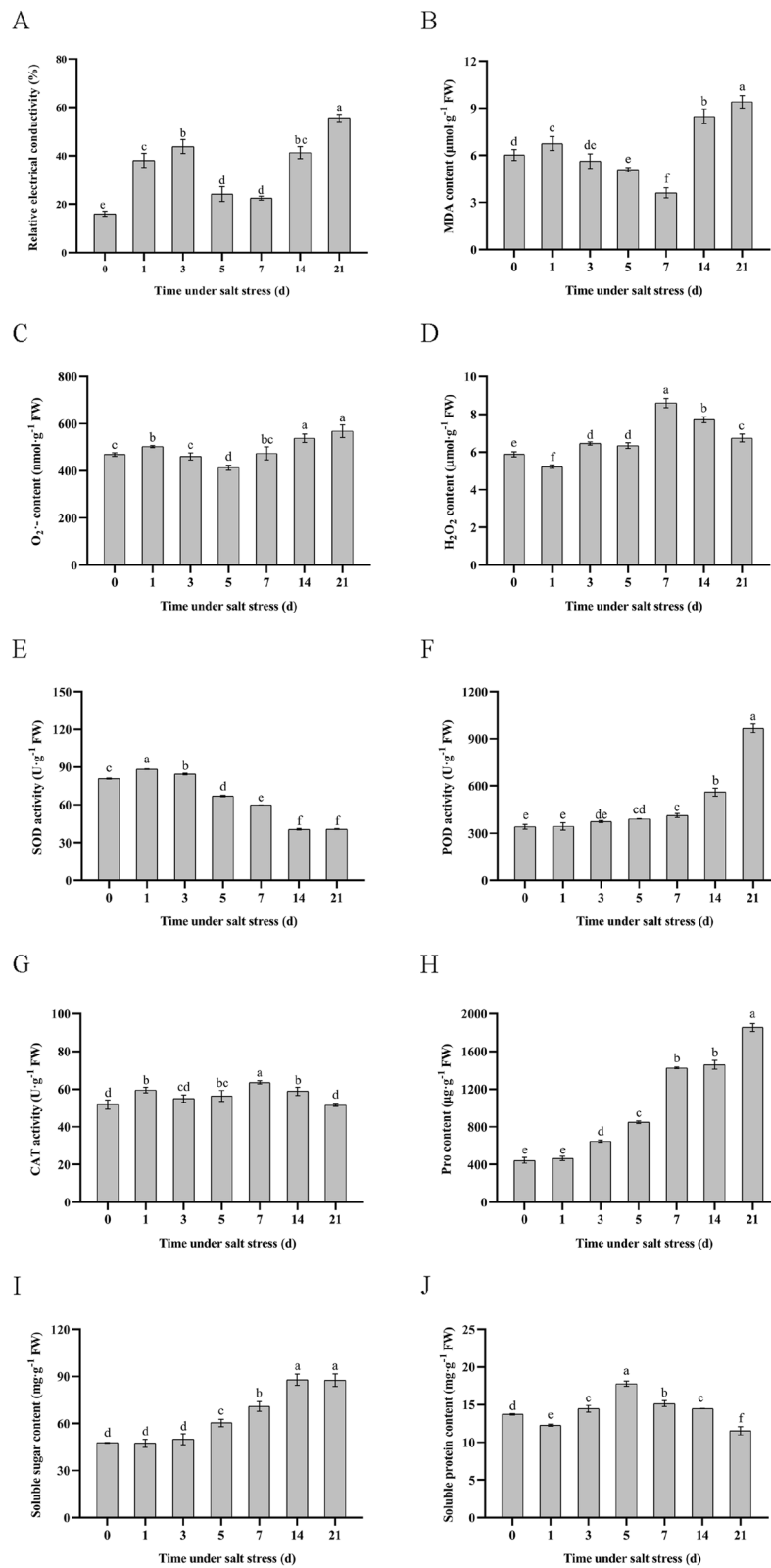


Fig. 2 Effect of Salt Stress Treatment on the Physiological Characteristics of *A. cicer* L.. The REC (A), MDA (B), O₂^{-•} (C), H₂O₂ (D), SOD (E), POD (F), CAT (G), Pro (H), SS (I) and SP (J) activity were measured. All data are presented as means ± SE from three independent experimental replicates, different letters indicate significantly different at *P* < 0.05

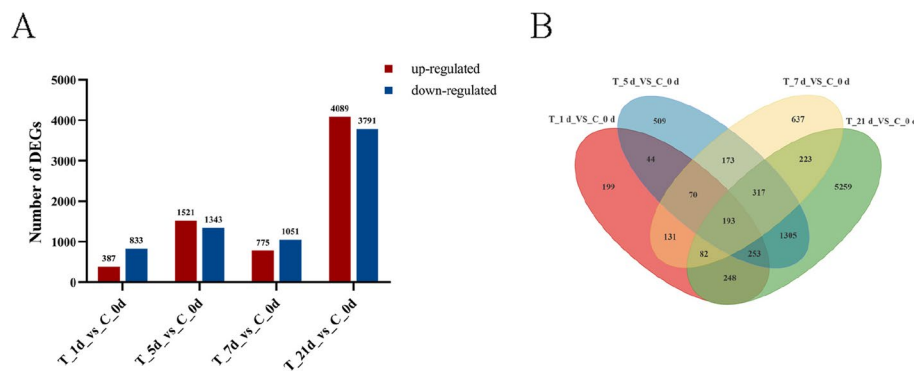


Fig. 3 Statistical analysis of differentially expressed genes (DEGs) in response to salt stress in *A. cicer* L.

and 43.19% GC content. Unigenes were assembled from scratch by using Trinity software, and the assembly results were evaluated. A total of 116,712 unigenes were obtained from 15 samples with a median length of 405 bp and an N50 length of 1,242 bp (Additional file 2: Table S2). The maximum length distribution of the unigenes was between 200 and 500 bp, with 68,517 bp, accounting for 58.71% of the unigenes (Additional file 2: Table S2 and Additional file 3: Figure S1).

Feature annotations of Unigenes

To obtain possible functional information on the Unigenes, six authoritative databases (NCBI-NR, GO, KEGG, Pfam, SwissProt, and eggNOG) were used for annotation. The results showed that the maximum number of annotations generated in the NR database accounted for 55.18%, while another 53.62%, 48.47%, 41.94%, 40.51%, and 17.65% of the unigenes were matched to the eggNOG, GO, Pfam, SwissProt, and KEGG databases, respectively (Additional file 4: Table S3).

Statistics and analysis of DEGs

The differentially expressed upregulated and downregulated genes were summarized by $|\log_2(\text{fold change})| \geq 1$ and $\text{FDR} < 0.05$ as the standard [1]. The expression of genes in *A. cicer* L. significantly changed after different NaCl stress treatments, and the number of genes whose expression changed varied. Compared with those in the control (C_0 d), 387 DEGs were upregulated and 833 were downregulated after 1 d of NaCl stress treatment; 1,521 DEGs were upregulated and 1,343 DEGs were downregulated after 5 d of treatment; 775 DEGs were upregulated and 1,051 DEGs were downregulated after 7 d; and 4,089 and 3,791 DEGs were upregulated and downregulated after 21 d, respectively (Fig. 3 A). The Venn diagram was constructed to display the number of unique and shared DEGs at different processing times, a total of 193 DEGs were common to the four treatment

time points, 199 DEGs appeared at only 1 d, and 509 DEGs appeared at only 5 d of treatment. In addition, 637 and 5,259 DEGs were specific to the 7 d and 21 d NaCl stress treatments, respectively (Fig. 3B).

GO functional enrichment analysis of DEGs

All DEGs were mapped to the entries of the GO annotation results, and all DEGs were categorized into three categories: “biological processes”, “cellular components”, and “molecular functions” (Additional file 5: Figure S2A). Based on the corrected p value, the top 20 entries were selected for enrichment analysis, and the main enriched terms for all DEGs were “photosynthesis”, “chloroplast”, “response to water deprivation”, “response to abscisic acid”, and “DNA binding transcription factor activity” (Additional file 5: Figure S2B).

KEGG pathway enrichment analysis of DEGs

The DEGs were mapped to the reference canonical pathways. Among the enriched DEGs in the KEGG database, the top 20 pathways were “plant hormone signal transduction (ko04075)”, “starch and sucrose metabolism (ko00500)”, “carbon fixation in photosynthetic organisms (ko00710)”, “flavonoid biosynthesis (ko00941)” and “thiamine metabolism (ko00730)” (Additional file 6: Figure S3).

Construction of the *A. cicer* L. coexpression network in response to salt stress

Based on the gene expression data and physiological index response data of *A. cicer* L. after salt stress, we conducted weighted gene coexpression network analysis (WGCNA) and found that the soft threshold in the network was ‘power=18’ (Additional file 7: Figure S4). The imported gene data were optimized and merged to finally obtain 16 modules, of which the MEturquoise, MEblue, MEbrown, MEyellow and MEgreen modules contained

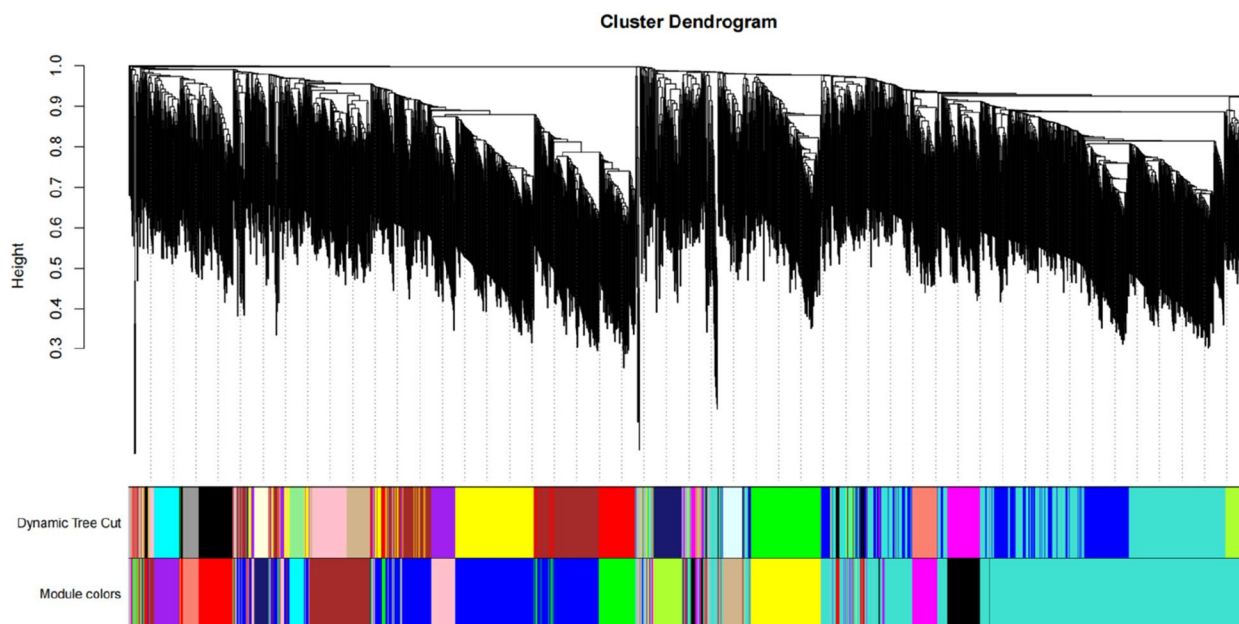


Fig. 4 Cluster dendrogram and module partitioning of genes. ‘Dynamic Tree Cut’ represents initial modules, ‘Module colors’ represent final modules; each branch in the hierarchical tree or each vertical line in color-bars represents one gene; genes not attributed to any module would be colored by grey

more specific genes (Fig. 4). We analyzed the correlations among modules and found that the MEgreen module was significantly correlated with the MEblue, MEpink and MEBrown modules; the MEBrown module was significantly correlated with the MEpurple, MERed and MESalmon modules; the ME midnightblue module was significantly correlated with the MEyellow and MECyan modules; and the METan module was significantly correlated with the METurquoise, MEblack and MEMagenta modules (Additional File 8: Figure S5). In addition, the correlation analysis revealed a significant positive correlation ($R > 0.5$, $P < 0.05$) or negative correlation ($R < -0.5$, $P < 0.05$) between the METurquoise, MEBrown, MEblue, MEgreen, and MEpink modules and most indicators, such as SOD, Pro, SS, H_2O_2 and POD (Fig. 5). In summary, the METurquoise, MEgreen, MEblue and MEpink modules were selected as key modules for further analysis and mining.

KEGG enrichment pathway analysis of key module genes

Through KEGG pathway enrichment analysis of genes in the METurquoise, MEgreen, MEblue, and MEpink modules, we found that there were genes enriched in the “plant hormone signal transduction (ko04075)” pathway in both the METurquoise and MEpink modules (Fig. 6A and D); the MEgreen and MEblue modules both had more genes enriched in “carbon fixation in photosynthetic organisms (ko00710)” and “carbon metabolism

(ko01200)” (Fig. 6B and C). Therefore, the “plant hormone signal transduction” and “carbon metabolism” pathways were used as the main targets for analysis.

Plant hormone signal transduction in *A. cicer* L. under salt stress

Visual analysis of the hub genes in the METurquoise and MEpink modules revealed that the key genes involved in the “plant hormone signal transduction” pathway in these two modules were *MKK1* (TRINITY-DN1966_c0_g1) in the ethylene signal transduction pathway (Fig. 7A) and *AcRRs* (TRINITY-DN1012_c0_g1) in the cytokinin signal transduction pathway (Fig. 7B).

Based on the $\log_{10}(TPM+1)$ values of enzymes and corresponding DEGs in the ethylene signal transduction pathway, a heatmap was constructed, and the results showed that most genes in the ethylene signal transduction pathway of *A. cicer* L. were highly expressed at 1 d and 7 d after salt treatment, but the number of highly expressed genes at 7 d was greater than that at 1 d; moreover, except for *ERF1/2*, the *ETR*, *CTR*, *SIMKK*, *EIN2*, *EIN3* and *EBF1/2* response regulator related genes all had multiple related genes with relatively high expression levels (Fig. 8). Therefore, the pattern of ethylene signal transduction pathway regulation in *A. cicer* L. after salt stress was as follows: the ethylene receptor *ETR* sensed the ethylene signal and induced high expression of some genes of the downstream receptor *CTR*, which activated

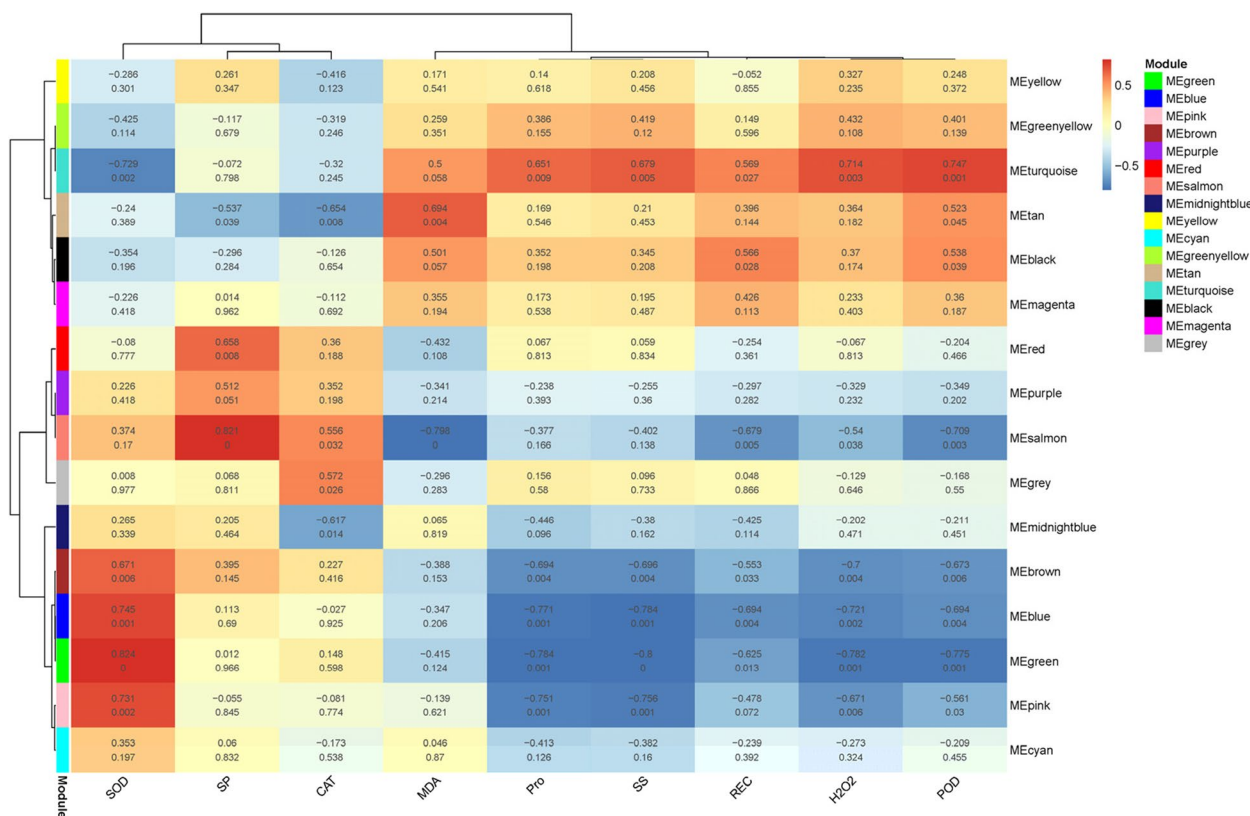


Fig. 5 Correlations between modules and trait. Each row represents one module, each column corresponds to a specific trait; the value above each cell at the row-column intersection represented the correlation coefficient (R) between the module and trait and was displayed according to the color of each cell; the value below the each cell represented the P -value, $P < 0.05$ indicated significant difference, $P < 0.01$ indicated extremely significant difference

the increase in the expression of the SIMKK, MPK6 and EIN2 response regulator related genes in the downstream cytoplasm, and then transmitted the signal to the EIN3 receptor in the nucleus. The high expression of most genes in EIN3 promoted an increase in the expression of the EBF1/2 genes, but the lower expression of the ERF1/2 genes influenced the subsequent transcription and translation of the genes related to the ethylene response (Fig. 8).

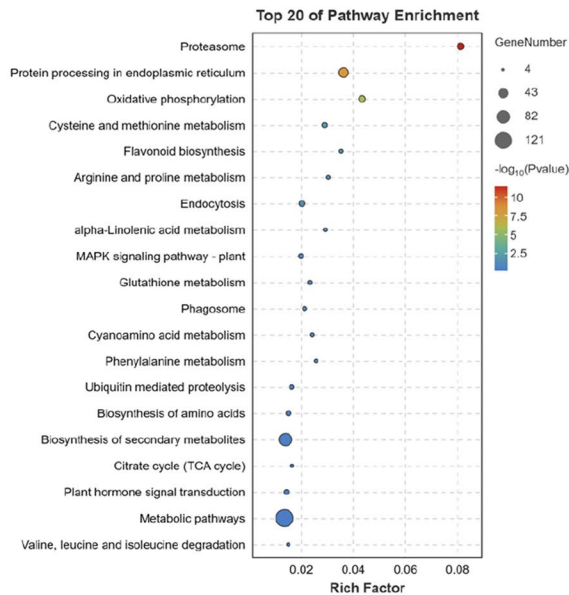
Similarly, analysis of the heatmap of the expression levels of enzymes and related genes in the cytokinin signaling pathway revealed that, similar to the ethylene signal transduction pathway, which was also highly expressed at 1 d and 7 d, the expression levels of most of the AHP and B-ARR genes increased in response to salt stress, and the expression of some CRE1 and A-ARR genes also increased (Fig. 9). Therefore, under salt stress, the cytokinin signal of *A. cicer* L. was transferred to the AHP protein by phosphorylation after being sensed by the transmembrane receptor CRE1, and the high expression of AHP-related genes caused the cytokinin signal to be positively transmitted to B class ARR. The high

expression of B-ARR genes not only activated the expression of the response factors of A class ARRs but also inhibited the activity of B class ARRs to maintain the balance of signal transduction processes and contributed to the expression of the downstream genes and transcription factors involved in the cytokinin response (Fig. 9).

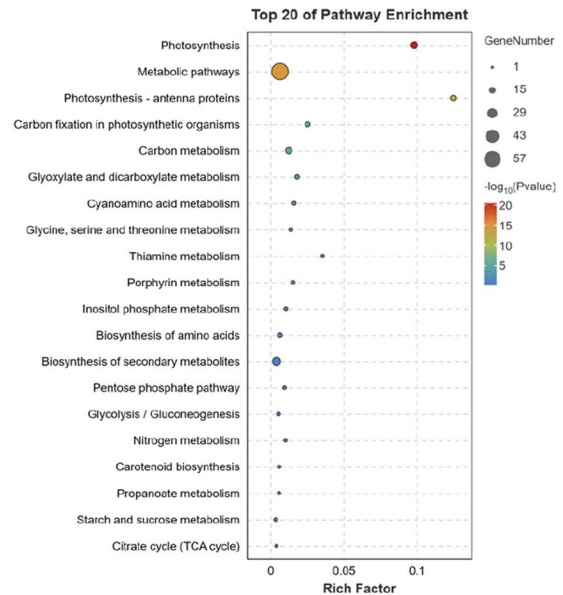
Carbon metabolism and related pathways under salt stress

Analysis of carbon metabolism in the MEGreen and MEBLue modules of *A. cicer* L. under salt stress revealed that a total of 41 genes were differentially expressed in this pathway, mainly distributed in the “Photorespiration (M00532)”, “Glycolysis (M00001)” and “TCA cycle (M00009)” of carbohydrate metabolism and the “Calvin cycle (M00009)” of carbon fixation metabolism, which are involved in the regulation of 17 key enzymes (Fig. 10). Based on the heatmap of TPMs, the expression peaks of these genes mainly appeared at 1 d, 0 d and 7 d; by clustering the genes at different treatment times, it was found that the expression levels of the genes at 1 d were similar to those at 0 d, 7 d and 5 d; and most of the genes were

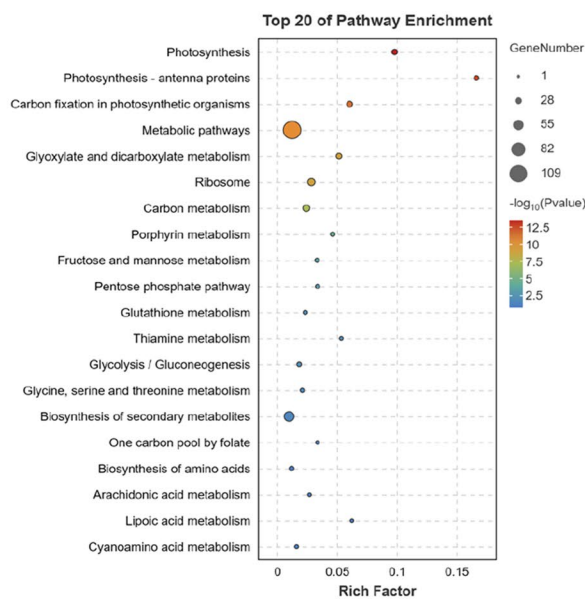
A



B



C



D

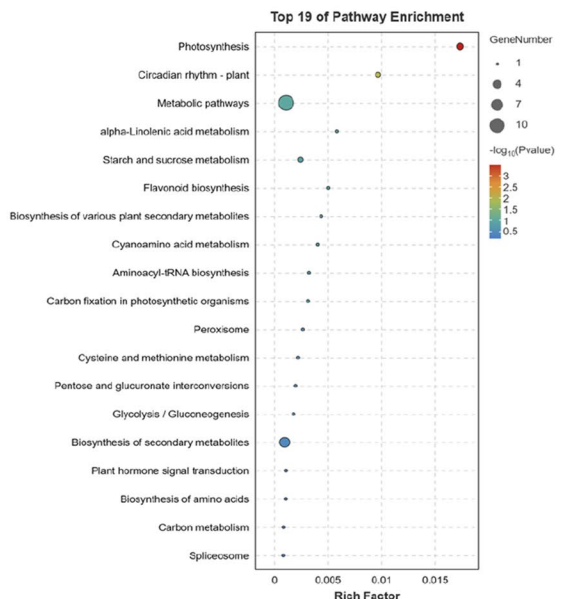


Fig. 6 KEGG enrichment analysis of genes in module module. **A:** Menturquoise module; **B:** MEgreen module; **C:** MEblue module; **D:** MEpink module

significantly reduced at 21 d, thus clustering into one group separately (Fig. 10).

Visualization of the hub genes in the MEgreen and MEblue modules revealed that the key genes involved in the above four carbon metabolic pathways were *PGK* (TRINITY_DN2162_c0_g2), encoding phosphoglycerate

kinase (PGK); *GAPA* (TRINITY_DN66_c0_g2), encoding glyceraldehyde-3-phosphate dehydrogenase (GADPH) in the glycolysis pathway; *PRK* (TRINITY-DN3867_c0_g1), encoding phosphoribokinase (PRK); and *rbcS* (TRINITY-DN53050_c0_g1), encoding ribose-diphosphate carboxylase (RBC) in the Calvin cycle; and *HAO*

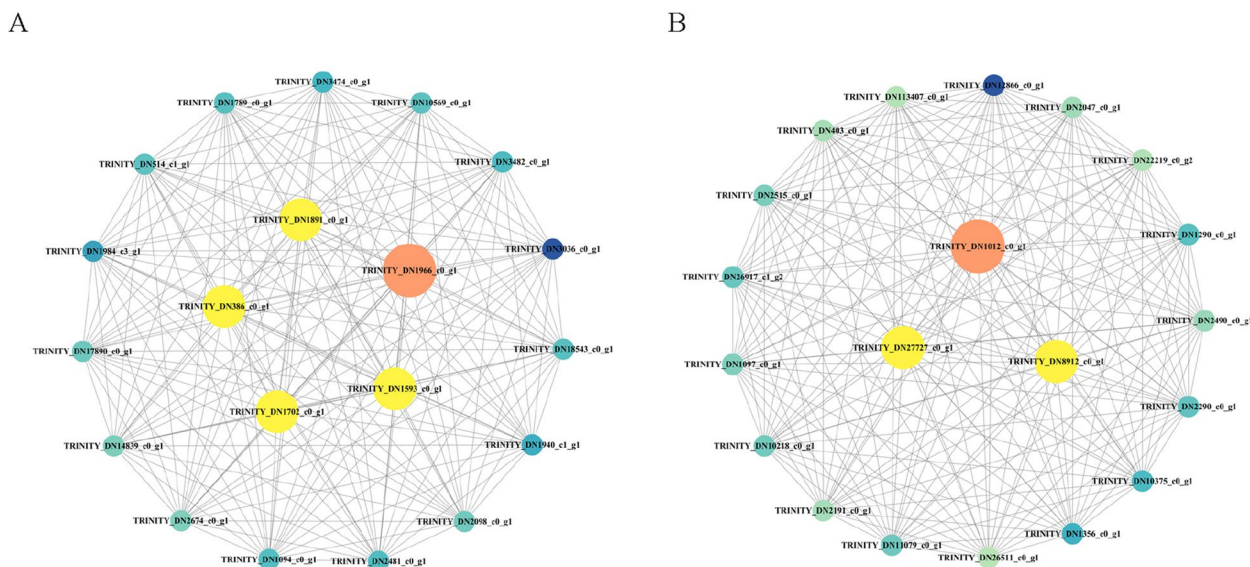


Fig. 7 Co-expression network analysis of hub gene in modules related to 'Plant hormone signal transduction'. **A:** METurquoise module, **B:** MEpink module; the red gene nodes represent genes related to 'Plant hormone signal transduction'; the yellow gene nodes represent genes with greater connectivity with red gene nodes; the blue gene nodes represent other genes connected with red gene nodes, the darker nodes represent more connections to other nodes, the lighter nodes represent fewer connections. The line between nodes indicate the coexpression between them

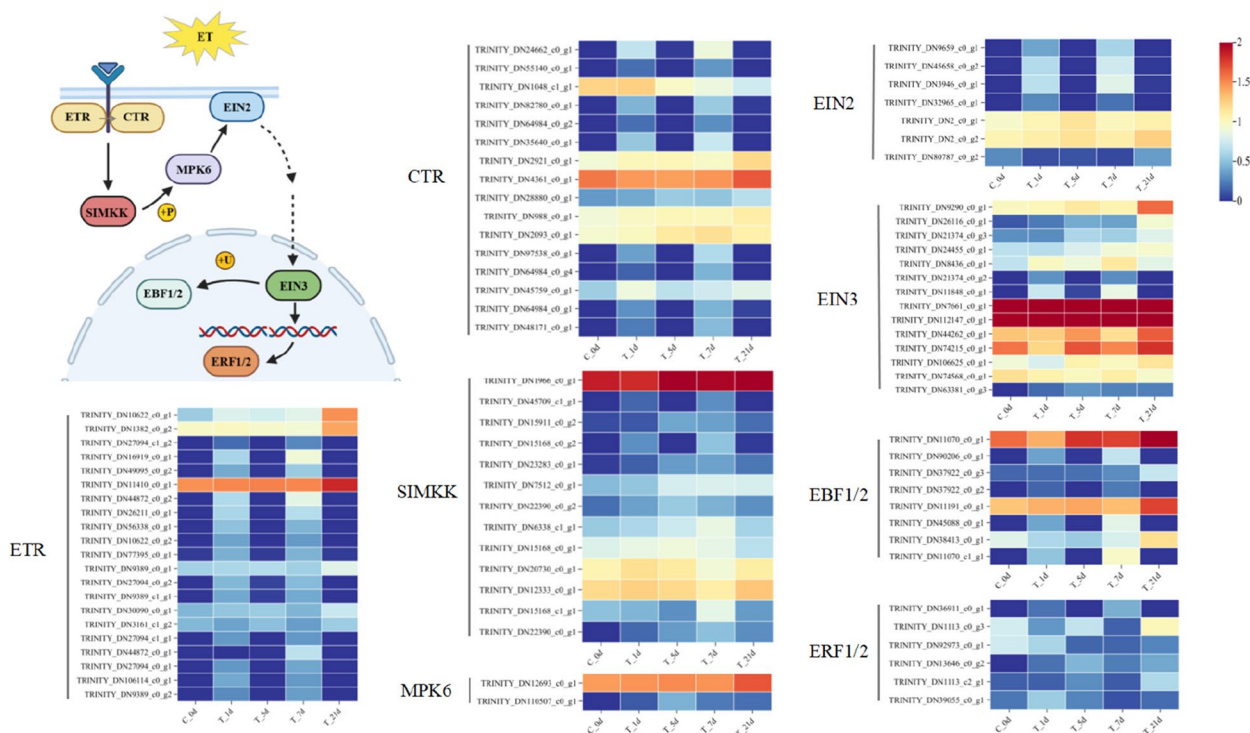
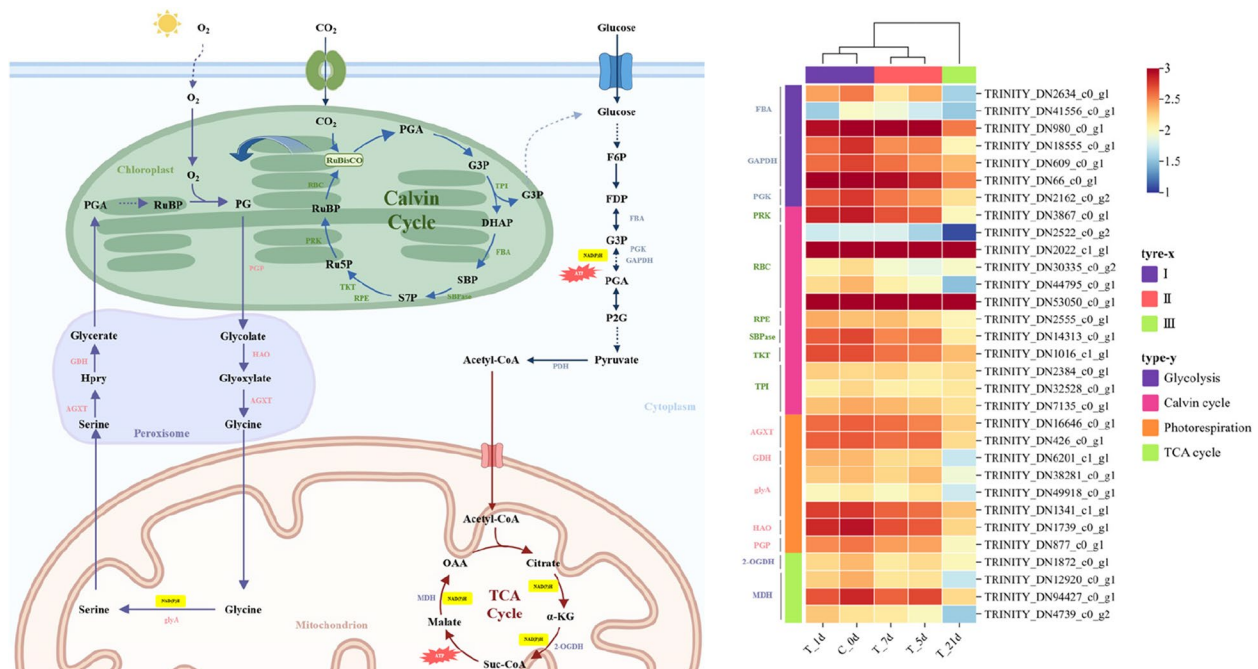
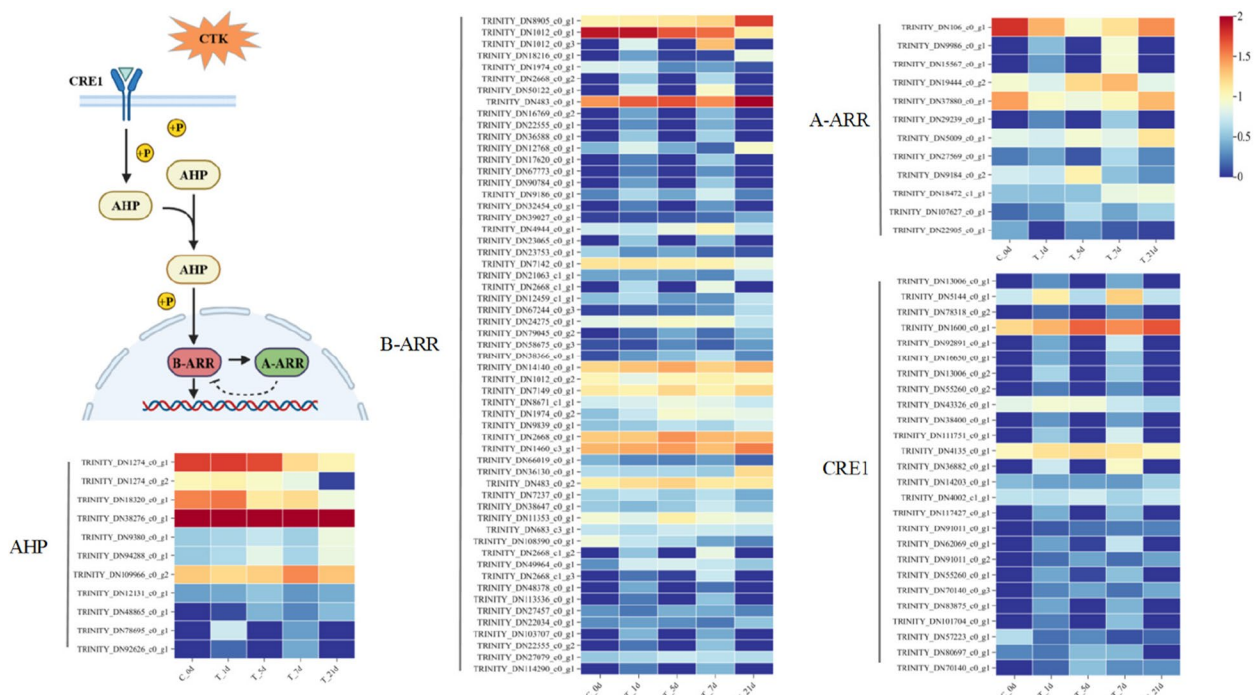


Fig. 8 Analysis of ethylene signaling pathway under salt stress. The display of gene expression in a heatmap, with blue to red indicated gene expression from low to high. The gene names corresponding to each gene ID are given in Additional file 10: Table S5



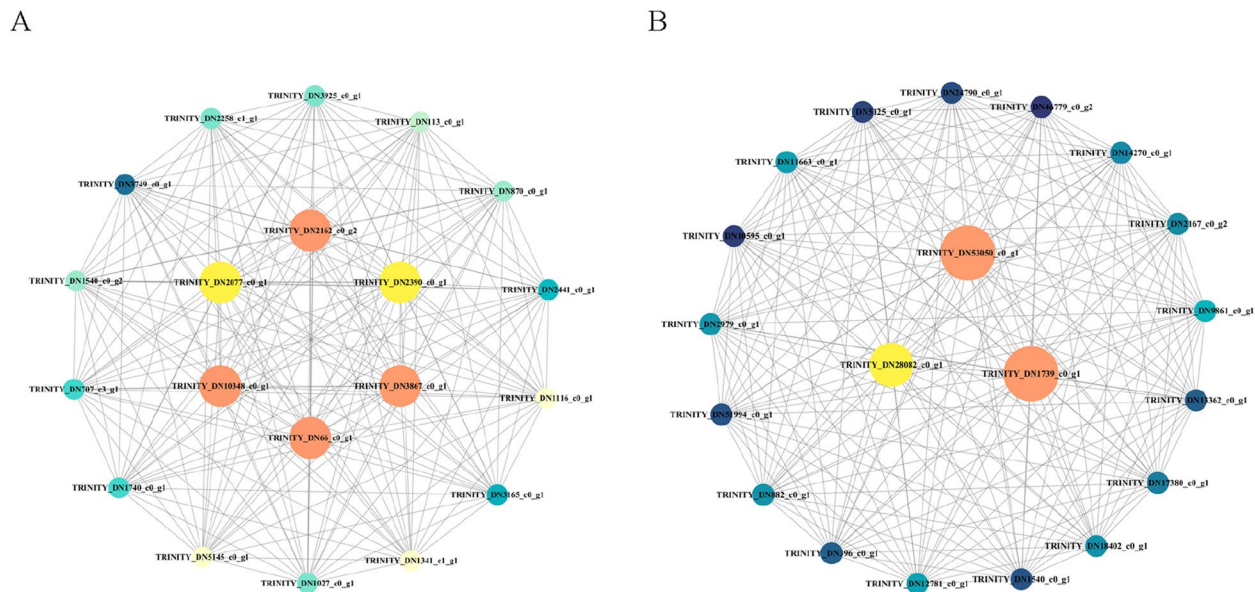


Fig. 11 Coexpression network analysis of hub gene in modules related to 'Carbon metabolism'. **A** MEgreen module, **B** MEblue module; the red gene nodes represent genes related to 'Carbon metabolism'; the yellow gene nodes represent genes with greater connectivity with red gene nodes; the blue gene nodes represent other genes connected with red gene nodes, the darker nodes represent more connections to other nodes, the lighter nodes represent fewer connections. The line between nodes indicate the coexpression between them

(TRINITY-DN1739_c0_g1), encoding hydroxy acid oxidase (HAO) during photorespiration (Fig. 11).

Validation of qRT-PCR for transcriptome analysis

To verify the reliability of the RNA-seq results and speculate about the mechanism of the response to salt stress in *A. cicer* L., qRT-PCR analysis was performed on 8 DEGs in the carbon metabolism pathway, 4 DEGs in the cytokinin signaling pathway, and 6 DEGs in the ethylene signaling pathway (Additional file 9: Table S4); the results showed that the expression patterns of 18 DEGs identified via qRT-PCR analysis were similar to those identified via transcriptome sequencing (Fig. 12). Through the linear correlation analysis between qRT-PCR results and RNA-seq results of each gene with different processing time, the results showed that the R^2 of 80% genes were greater than 0.8, showing a good correlation, which further confirmed the reliability of RNA-seq data (Fig. 12).

Discussion

Salt stress is one of the major abiotic stresses affecting plant growth and distribution [1]. Salt ion stress is often sensed first by the cell membrane, and the enrichment of ions causes oxidative damage to the cell membrane structure, increased permeability, and extravasation of intracellular electrolytes, leading to an increase in the REC and MDA content [26]. In the salt stress adaptation strategy of plants, the synthesis and accumulation of osmoregulatory substances such as Pro, SS, SP, betaine

and PAs are induced, thereby reducing the cellular osmotic potential, reducing water loss under short-term osmotic stress, enhancing cell expansion and cell scaling under long-term stress, and stabilizing cell structure [27, 28]. Salt stress-induced stomatal closure limits photosynthesis and enhances ROS production [29], and low ROS concentrations can be used as a signal to activate the salt stress response; conversely, high concentrations of active ROS can damage proteins, lipids, DNA, and carbohydrates [30]. SOD is the most effective ROS scavenger in the antioxidant enzyme system, serving as the first line of defense against ROS damage under environmental stress by converting $O_2^{\cdot-}$ to H_2O_2 , which is further detoxified into H_2O through CAT, POD, and ascorbate peroxidase (APX, EC.1.11.1.11), leading to the scavenging of ROS and the control and repair of damage [31]. In this study, the effects of salt stress on the REC, MDA, and ROS in the leaves of *A. cicer* L. were relatively small in the early stage and decreased in the middle stage; however, the increase in the content of these substances in the leaves in the later stage led to plant wilting (Fig. 2A, B, C and D). The antioxidant enzymes SOD, POD and CAT, as well as the osmotic regulators Pro, SS and SP, maintained a relatively stable state in the early stage and showed an upward trend in the later stage, except for SOD. The reason may be that under long-term salt stress, plants produce lipid peroxidation, which destroys the integrity of the intimal system and organelle function, resulting in irreversible damage to the cell membranes [32].

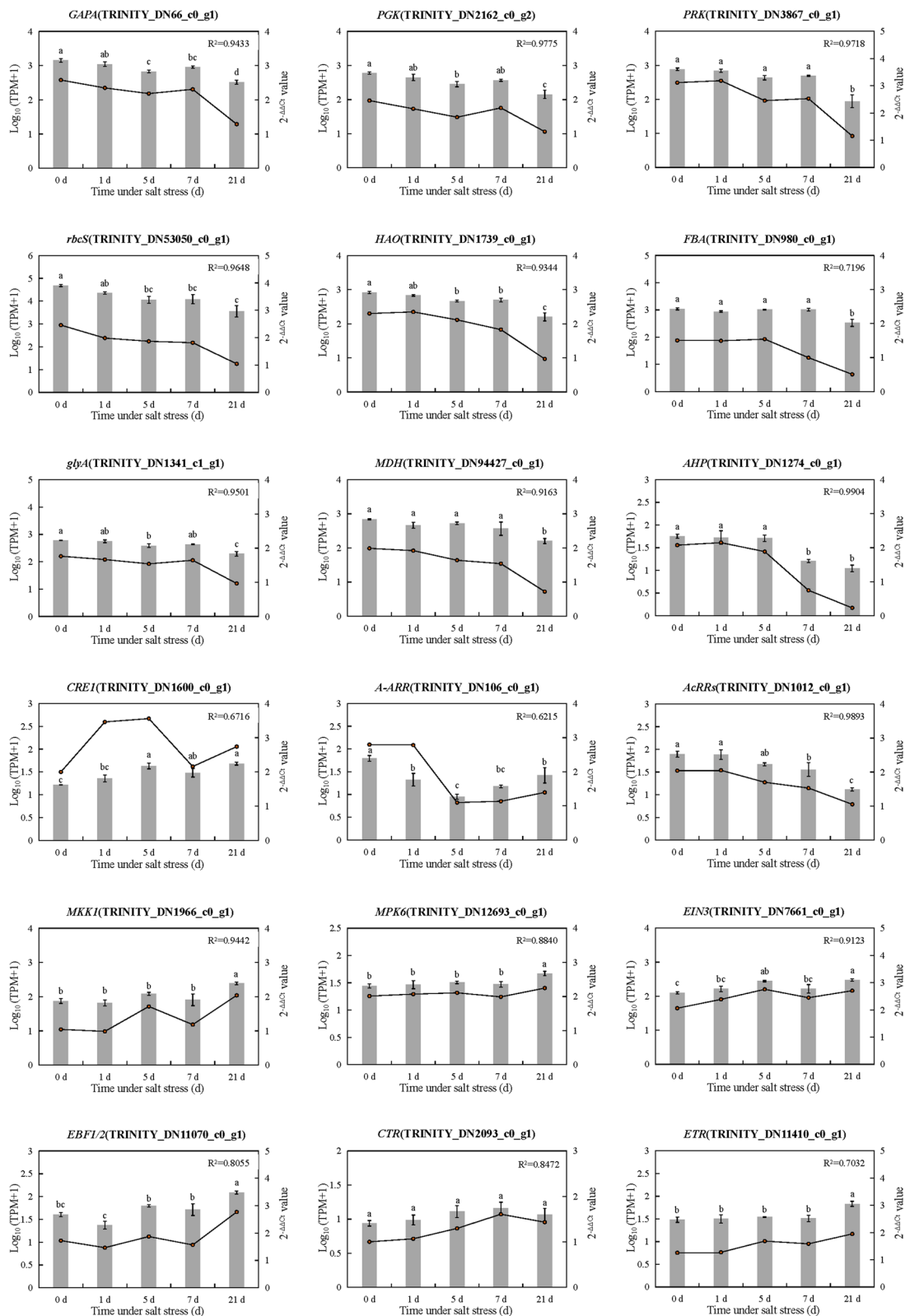


Fig. 12 qRT-PCR validation of transcriptome analysis. R^2 means the correlation between RNA-seq results and qRT-PCR results of genes under different salt stress times

In addition, metabolic dysregulation in the late stage of salt stress induce a toxic accumulation of ROS to produce toxicity effect and reduce SOD activity [29]. All of the above findings showed that antioxidant enzymes and osmotic substances were actively participated in the response to salt stress in the leaves of *A. cicer* L..

Cytokinins are involved in the regulation of a series of physiological processes in plants, such as cell division, stomatal opening, chloroplast development, leaf senescence, legume nodule formation and response to abiotic stresses, and play a crucial regulatory role in plant growth and development [33, 34]. Plants respond to cytokinin through the two-component signaling pathway, which is sensed by His kinase receptors (AHK1-4, WOL1, CRE1, and CRF) and triggers multistep phosphorylation, which delivers phosphate to class B or class A response regulators (ARRs) through phosphotransferase proteins (AHPs) to trigger the cytokinin response [35]. In this study, the expression levels of most genes regulating the response regulator AHP, B-ARR, CRE1 and A-ARR in cytokinin transduction pathway changed after salt stress (Fig. 9); therefore, the cytokinin transduction pathway was closely related to the response of *A. cicer* L. to salt stress. Yin et al. [36] reported that the A-type response regulator *ZmRR1* regulated the exclusion of Cl^- from maize stems, which is the basis for the natural variation in maize salt tolerance. However, in this study, the hub genes in the specific module were visualized, and two-component response regulator *AcRRs* involved in the regulation of B-ARRs were found to be specifically expressed during salt stress in *A. cicer* L. (Fig. 7B). Normally, after the cytokinin signal is transmitted from the membrane to the nucleus, B-type ARR positively regulate cytokinin signal transduction by regulating the transcription of downstream genes [37], whereas A-type ARR negatively regulate cytokinin signal transduction by interacting with HPs and inhibiting their function; moreover, when A-type ARR are activated, they inhibit the activity of B-type ARR to affect signal transduction [38]. B-type ARR play a crucial role in the early response of plants to cytokinins, regulating root and shoot conduit development, photosensitivity, chlorophyll production, hypocotyl elongation, and cell division [39]. One study has found that B-type response regulators *ARR1* and *ARR12* regulate Na^+ accumulation in aboveground parts of plants by encoding high affinity K^+ transporters [40]. Nguyen et al. [41] also reported that *Arabidopsis thaliana* lines transformed with *ARR1*, *ARR10* and *ARR12* exhibited significantly greater drought tolerance than did WT plants and that their enhanced drought tolerance may be related to enhanced cell membrane integrity, increased anthocyanin biosynthesis, increased abscisic acid (ABA) hypersensitivity and reduced stomatal aperture. Therefore, in

our study, the good salt tolerance of *A. cicer* L. seedlings in the early stage may be related to the positive regulation of cytokinin signaling by B-ARRs.

Ethylene is an important signaling molecule in the plant response to abiotic stress, and stress-induced ethylene production is sensed by ethylene receptors and triggers downstream cellular responses through the ethylene signal transduction pathway [42]. The ethylene signaling pathway involves the ETR of ethylene receptors, CTR, SIMKK, EIN2, EIN3 and other components [43]. Previous studies have shown that ethylene signaling plays a positive regulatory role in plant resistance to salt stress by studying mutants of the key membrane localization proteins *ETR1* and *EIN2* in *A. thaliana* [44]. This study revealed that during the occurrence of salt stress, the ethylene signaling pathway of *A. cicer* L. was upregulated by only a few *ERF1/2*-related genes, while multiple related genes, such as *ETR*, *CTR*, *SIMKK*, *EIN2*, *EIN3*, and *EBF1/2*, exhibited high expression levels, indicating that salt stress activated the response of the ethylene signaling pathway. *EBF1/2* is an F-box protein 1 and 2 commonly present in plants that negatively regulates the ethylene signaling pathway by mediating the degradation of the EIN3 protein [45], controlling many key processes in plants, such as hormone response, seed germination, seedling development, lateral root formation, and abiotic stress response [46]. Guo et al. [47] reported that overexpression of the *SIEBF2* gene promoted the nutritional growth of tomato plants and strongly delayed fruit development and ripening. The ethylene response factor (ERF) protein enhances tolerance to environmental stress by regulating the biosynthesis of plant metabolites such as jasmonate, gibberellin, ethylene and lipids [48, 49]. Zhang et al. [50] found that the ectopic expression of *GmERF3* gene isolated from *Glycine max* into tobacco plants not only induced the expression of some PR genes, enhanced the resistance of plants to biological stress, but also gave them the tolerance to high salinity and dehydration stress. However, some studies have found that under normal environment, plant ethylene content was low, while under salt stress, ethylene synthesis increased, accelerating leaf senescence and abscission, causing plant death [51]. Therefore, in this study, only a few *ERF1/2* related genes were upregulated during salt stress (Fig. 8), which may also be related to promote the cytokinin accumulation in leaves and reduce the content of salt ions in leaves by salt stress, thus inhibiting the positive regulation of ethylene synthesis signal and slowing down the senescence of leaves. Extracellular stimuli are perceived by plasma membrane receptors and activate the mitogen-activated protein kinase (MAPK) cascade through sequential phosphorylation of MAPK [52]. Studies have shown that in plants, *MKKs* positively regulate ethylene

biosynthesis by activating MPKs [53]. Our study revealed that the expression level of *MKK1* in the ethylene signaling pathway increased with increasing salt stress time in the early stage but decreased at 7 d of salt stress (Fig. 8). Previous research has shown that *MKK1*, *MKK2* and *MKK3* mediate the MAPK signaling cascade response to plant salt tolerance by participating in transcriptional regulation, ABA signal transduction, cellular defense, and stress metabolism during plant salt stress [54, 55]. The plant hormone ABA induces the expression of plant resistance genes through complex signaling cascades, thereby tolerating environmental stress factors such as cold, drought, and salt. Xiong et al. [56] reported that overexpression of *OsMAPK5* could enhance plant tolerance to drought, salt, and cold stress, and the addition of exogenous ABA to rice could also induce high expression of the *OsMAPK5* gene and its protein and enzyme activity in cells, thereby positively regulating drought, salt, and cold tolerance and negatively regulating the expression of disease progression-related (PR) genes. The ethylene receptor *ETR* is also a part of the His kinase receptor family [57], previous reports have shown that the ethylene receptor *ETR1* interacts with several His-containing phosphate transfer (AHP) and ARR proteins in the cytokinin pathway, causing phosphate transfer from the ethylene receptor to the cytokinin pathway to regulate plant responses [58]. Mutation of the ethylene receptor *ETR1* gene reduced the ethylene response, resulting in increased dormancy and delayed germination, as well as increased ABA inhibition, but the addition of the cytokinin N-6 benzyladenine (BA) reversed the sensitivity of *A. thaliana* mutants to ABA [59]. These findings indicated that the role of cytokinin in promoting germination was at least partially related to the production of ABA and ethylene. In addition, ethylene receptors *ETR1* and *ETR2* have also been confirmed to be independent of ethylene signal, affecting ABA signal and cytokinin signal transduction and causing germination changes during salt stress [60]. Under drought stress, it was also observed that genes related to ethylene and ABA signal transduction were significantly induced in the leaves of *Ammopiptanthus mongolicus*, and as a unique ethylene response factor of the plant, its ectopic expression significantly improved the drought tolerance of transgenic plants [61]. Therefore, in this study, the regulatory effect of promoting the cytokinin pathway and inhibiting the ethylene signaling pathway in the early stage of salt stress in *A. cicer* L. may also be related to the ABA signaling pathway; therefore, the mechanism by which ABA influences and interacts with ethylene and cytokinin to control the response of *A. cicer* L. to salt stress still needs further research.

In plants, carbon metabolism is closely related to other metabolic pathways and is sensitive to environmental stress; carbon not only provides the necessary carbon source and energy for plant growth and development but also produces signaling molecules such as sucrose and glucose to act on downstream transduction pathways [62]. The increase in soil osmotic pressure caused by salt stress makes it difficult for plants to absorb water and nutrients and induces stomatal closure to reduce the net photosynthetic rate [63]. In addition, salt stress can also damage chloroplast structure and the photosynthetic membrane system, leading to a weakening of carbon sequestration in the Calvin cycle and a decrease in carbon assimilation capacity [64]. The Calvin cycle occurs in the chloroplast matrix, which is the basic carbon assimilation process of both C3 and C4 plants; through this pathway, green plants reduce and fix CO₂ to triose phosphate or hexose phosphate, which are used as substrates for respiration and participate in other metabolic reactions [65, 66]. One study reported that the upregulated expression of the protein CBL-interacting protein kinase (CIPK) of the Ca²⁺ signaling pathway in halophytes significantly increased the expression of genes encoding GAPDHs and Rubisco in the Calvin cycle in plants [67]. In this study, we also found that the expression of the hub genes *PRK* and *rbcS* in the Calvin cycle of *A. cicer* L. remained relatively stable from 1 to 14 d of salt stress but decreased at 21 d of salt stress (Figs. 10 and 11). *PRK* and *rbcS* rely on ATP to catalyze the phosphorylation of ribose-5-phosphate (Ru5P) to ribose-1,5-phosphate (RuBP) and the carboxylation of Rubisco to synthesize 3-phosphoglycerate (PGA) in the Calvin cycle, which is a key step in the regeneration phase of the Calvin cycle [68]. High expression of the *PRK* and *rbcS* genes can significantly improve the carboxylation of Rubisco and the regeneration of RuBP, thereby enhancing the photosynthesis of tomato plants [69]. These results indicated that the expression levels of these genes regulate the photosynthetic capacity of plants; therefore, short- and medium-term salt tolerance in this study may have decreased the photosynthetic ability of *A. cicer* L. The glycolysis pathway is an important carbohydrate metabolism pathway that decomposes hexose into pyruvate and releases energy [70]. After pyruvate, the end product of glycolysis, enters the mitochondria, the tricarboxylic acid cycle (TCA cycle) finally oxidizes carbohydrates to CO₂ and water through a series of physiological and biochemical reactions and releases the energy required for biological activities [71]. Through visual analysis of hub genes in the MEgreen and MEblue modules, our study revealed that *PGK* and *GAPA*, involved in the glycolysis pathway, were differentially expressed, and the expression levels of the *2-OGDH* gene encoding 2-oxoglutarate

dehydrogenase and MDH-related genes encoding malate dehydrogenase in the TCA cycle also changed at the time of salt stress and were significantly greater than those at 21 d (Figs. 10 and 11). The photosynthetic capacity of crops is highly regulated by GAPA, and exists in *Pisum sativum*, *Vicia faba*, *Phaseolus vulgaris* and other legumes to promote the redox regulation level of GAPDH activity in the form of homologous tetramer A4 or heterotetramer A2B2 [72]. Existing studies have confirmed that PGK exists in the cytosol and plastid, one of which may participate in photosynthesis and the other in glycolysis in the form of GAPDH subtype [73]. In addition, the determination of the functional localization signal of pea PGK in the leaf nucleus also showed that PGK may act as moonlighting proteins, which not only participate in metabolism, but also play a role in abiotic tolerance [74, 75]. Wu et al. [76] reported that the GAPA1 and PGK1 proteins in *A. thaliana* interact with the enolase-encoded protein ENO2, which catalyzes the dehydration of 2-phosphate-D-glycerate (2-PGA) to phosphoenolpyruvate (PEP), thereby regulating the expression of plant hormone signal transduction pathways, stress response factors and ROS-related genes and proteins under salt stress and subsequently affecting seed germination. In addition, Wang et al. [77] reported that the overexpression of MDH in apple leaves could change the metabolism of mitochondria and chloroplasts and increase the levels of reducing power, ascorbic acid, glutathione and salicylic acid (SA), increasing the salt tolerance and cold tolerance of transgenic apple plants. 2-OGDH catalyzes the oxidative decarboxylation of 2-oxoglutarate (2-OG) to succinyl-CoA in the TCA cycle, and its regulatory role includes the allosteric reaction of the second messenger Ca^{2+} and ATP/ADP, NADH/NAD, acetyl-CoA and other metabolic indicators, playing a role in regulating plant growth in a highly interactive manner [78, 79]. Studies have shown that phosphorus deficiency can reduce the content of the 2-OGDH cofactor thiamine diphosphate (ThDP) in aboveground tissues and roots [80]. Because ThDP is an essential 2-OGDH cofactor, insufficient ThDP levels prevent 2-OG from being oxidized to succinyl-CoA by 2-OGDH, thus limiting circulation flux and cell respiration in the TCA cycle [81]. Accordingly, this finding also proves that the glycolysis pathway and its downstream TCA cycle play important roles in the response to abiotic stress in plants. Photorespiration is a reaction involving Rubisco, a product of the Calvin cycle. Green plant cells use light energy to absorb O_2 and release CO_2 [82]. Under conditions of water deficit or high light, the stomata of leaves are closed, and the CO_2 released by photorespiration can be fixed, which can protect the reaction center of photosynthesis from being damaged by strong light [83]. As a key enzyme of

photorespiration, hydroacid oxidase converts glycolate to glyoxylate; studies have shown that the gene *IHAOX*, encoding the enzyme, is highly active in autotrophic and heterotrophic organs and is involved in the metabolism of serine and fatty acids or amino acids [84]. One study reported that increasing photorespiratory capacity may reduce the negative feedback of photorespiratory metabolites on the Calvin cycle, thereby enhancing CO_2 assimilation [85]. Hoshida et al. [86] studied the potential role of photorespiration in preventing salt stress in transgenic rice and confirmed that the enhancement of photorespiration endows rice plants with salt resistance. Our study revealed that the expression of the *HAO* gene in *A. cicer* L. after 21 d of salt stress was significantly lower than that after 21 d of salt stress (Fig. 10), which indicates that the *HAO* gene also regulates the response of *A. cicer* L. to salt stress via positive feedback.

Interestingly, among the four key modules of this study, both the carbon metabolism pathway and the plant hormone signaling pathway were specifically involved in the response of *A. cicer* L. to salt stress. Carbohydrates can be integrated into the plant hormone pathway as signal molecules and interact with plant hormones such as ABA, ethylene, cytokinin and gibberellin [87]. During the germination of plant seeds, carbohydrates can be used as regulators of ABA synthesis-related gene activation to jointly improve the germination rate [88]. Ethylene can antagonize the inhibitory effect of high concentrations of sugars on seed germination [87], and cytokinins reduce the accumulation of carbohydrates by inducing the transformation of enzymes, thus making full use of carbohydrates and ultimately delaying aging [89]. This further indicates that there may be some connection between the carbon metabolism pathway and plant hormone signaling pathway in response to abiotic stress in plants, and the specific response mechanism needs to be further studied.

Conclusions

In this study, we conducted a comparative transcriptomic analysis of *A. cicer* L. under salt stress and performed WGCNA combined with a physiological response analysis. We found that the physiological response of *A. cicer* L. to salt stress was closely related to four modules, and KEGG analysis of key modules revealed that plant hormone signal transduction and carbon metabolism were significantly enriched. In addition, the hub genes of these two pathways were identified, and the *AcRRs* of the cytokinin signal transduction pathway, *MKK1* of the ethylene signal transduction pathway and *PGK*, *GAPA*, *PRK*, *rbcS* and *HAO* of the carbon metabolism pathway were shown to play important roles in the regulation of salt stress in *A. cicer* L.. Although more studies are needed to discover

the mechanism of the response to salt stress in *A. cicer* L., this study has preliminarily identified many candidate genes that can be used in salt tolerance breeding, providing new gene sources for germplasm innovation in *A. cicer* L..

Methods

Cultivation of seedlings and salt stress treatment

Seeds of uniform size of *A. cicer* L. 'Ganlv 2' (stored in the herbarium of the college of grassland science, Gansu agricultural university; bred variety Registration No.: Guo S-BV-AC-002-2021, applicant: Gansu Chuanglv Grass Industry Technology Co., Ltd and Gansu Agricultural University) were selected and evenly sown in a nursery bowl (10×10×12 cm) after disinfection with 10% NaClO and 75% alcohol. The substrate in the seedling bowl was high-temperature and high-pressure sterilized sand. When the seedlings grew their first true leaf, they were transplanted to a hydroponic box (12×9×12 cm) containing Hoagland's nutrient solution. Each hydroponic box included 12 plants, which were subsequently placed in an artificial climate incubator for cultivation at a day/night temperature of 25±1°C, a light/dark cycle of 16 h/8 h, a light intensity of 5000 lx, and a humidity of 50%-70%. Each group consisted of 6 boxes of seedlings, with 3 biological replicates for each group for the next step of the experiment. When the *A. cicer* L. seedlings grew to approximately 20 cm, 150 mmol·L⁻¹ NaCl stress treatment was applied. During the stress period, the lost water was supplemented in a timely manner with nutrient solution to ensure a constant salt concentration. Next, samples were taken at 0, 1, 3, 5, 7, 14 and 21 days after salt stress, and relevant physiological indicators were measured.

Determination of physiological indicators of *A. cicer* L.

Leaves were randomly collected from different samples of *A. cicer* L. plants, and 3 biological replicates were performed for each physiological indicator; 0.2 g of each replicate was collected, except for fresh samples for REC, and the other samples were quickly frozen in liquid nitrogen and stored in an ultralow temperature refrigerator at -80°C for physiological indicator measurement. The REC was measured by a conductivity meter [90], the MDA content was determined by the thiobarbituric acid method [91], the Pro content was determined by the sulfosalicylic acid extraction method [92], the SS content was measured using the anthrone method [93], and the SP content was measured by the Coomassie brilliant blue staining method [94]. SOD activity was measured using the nitrogen blue tetrazole colorimetric method [95], POD activity was measured

by the guaiacol method [96], and CAT activity was measured by UV colorimetry [97]. The rate of O₂⁻ production was determined by the hydroxylamine oxidation method [98], and the H₂O₂ content was measured using the UV spectrophotometer [99].

Extraction and quality testing of total RNA

The trends of most physiological indexes, such as REC, H₂O₂, POD, CAT, Pro, and SP, turned at 1, 5, 7, and 21 days of 150 mmol·L⁻¹ NaCl treatment. So based on the data changes of growth phenotypic characteristics and physiological and biochemical indexes of *A. cicer* L., we selected 0, 1, 5, 7, and 21 days of NaCl treatment as the main time points for transcriptomics sequencing. The Plant Total RNA Extraction Kit (Tianjin Biotech, Beijing, China) was used to extract total RNA from the leaves. Agarose gel electrophoresis (1.0%) was used to identify the degradation or contamination of the extracted RNA samples, an ultramicro spectrophotometer was used to evaluate the purity of the RNA, and an Agilent 2100 biological analyzer (Agilent, Palo Alto, MA) was used to detect the integrity of the RNA.

Library construction and Illumina sequencing

After qualifying the total RNA samples, eukaryotic mRNA was enriched with magnetic beads containing oligo (dT), and fragmentation buffer was added to break the mRNA into short fragments. The fragmented mRNA was used as a template, and cDNA was synthesized by six-base random hexamers, dNTPs, RNaseH, and DNA polymerase I. The double-stranded product was purified using AMPure XP beads. The sticky end of the purified double-stranded cDNA was repaired to a flat end, base 'A' was added at the 3' end, and the cDNA was connected to the sequencing adapter. AMPureXP beads were used for fragment selection, the second strand of cDNA containing 'U' was degraded, and PCR amplification was performed to obtain the final sequencing library. After quality inspection of the library, an Illumina NovaSeqTM 6000 was used for sequencing.

Sequence assembly and functional annotation

The raw data obtained from Illumina (deposited in NCBI, the accession number is PRJNA1079516) high-throughput sequencing were obtained by removing connector sequences and filtering out unqualified sequences to obtain high-quality and effective data (Clean data). Due to the lack of publicly available whole-genome sequencing information for *A. cicer* L., this study used Trinity software (v 2.15) to mix and assemble all the samples after obtaining the clean reads. After normalization, the unigenes were obtained and used as the basis for

subsequent bioinformatics analysis. Using DIAMOND software (v 2.0.15), the transcripts and unigenes obtained from transcriptome sequencing were functionally annotated with six authoritative databases (NCBI-NR, GO, KEGG, Pfam, SwissProt, and eggNOG) to obtain annotation information for each library. The NR, Pfam, SwissProt, and eggNOG datasets all retained the best match results (meeting the *E-value* threshold of 10^{-5} and retaining the annotation with the smallest *E-value*); the GO and KEGG databases retained all annotation results that met the set threshold (*E-value* $< 10^{-5}$).

Unigene differential expression analysis

The expression level of Unigenes was standardized using TPM, and difference multiple of $|\log_2(\text{fold change})| \geq 1$ and the false discovery rate (FDR) < 0.05 were used as the standards for identifying DEGs [1]. All significantly expressed DEGs were mapped to the GO annotation and KEGG annotation results of each entry (pathway) of unigenes, the number of unigenes for each entry (pathway) was calculated, and hypergeometric tests were applied to identify the enriched GO pathways and KEGG pathways in unigenes with significant differential expression (*P* value < 0.05).

Construction of the coexpression network module

The online tool ImageGP (<http://www.bic.ac.cn/BIC/#/>) was used for WGCNA [100]. The standardized gene expression data from 15 samples subjected to different salt stress treatments were input into a scale-free network dataset, and 9 sets of physiological indicator data processed at the same time as the transcriptome were imported as the phenotypic data for module association analysis. The soft threshold value was determined by the scale-free topology fit index curve, 'Pearson' test was used to calculate the correlation coefficient between the module and each phenotypic index, and the other parameters were set to their default values. The data were analyzed via the Majorbio Cloud Platform (<https://cloud.majorbio.com/page/tools/>) for GO and KEGG enrichment analysis of DEGs in the module [101]; the corrected *P* value was set at a threshold of 0.05 to determine the GO functions and KEGG pathways significantly enriched in the genes. At the same time, specific modules that were highly correlated with phenotypes were screened, and a weighted gene coexpression network diagram was drawn with Cytoscape (v 3.10.1).

Real-time quantitative PCR (qRT-PCR) verification

To verify the reliability of the transcriptome data, 18 DEGs were randomly selected for validation by qRT-PCR. The extraction method for total RNA was the same

as above, and the PrimeScript™ II 1st Strand cDNA Synthesis Kit (Solarbio, Beijing, China) was used to reverse transcribe RNA into cDNA. cDNA was used as the template, and the *actin* gene was used as the internal reference [102]. Real-time fluorescence quantitative analysis was performed with a LightCycle 96 real-time fluorescence quantitative PCR instrument (Roche, Basel, Switzerland), with 4 technical replicates included in the experiment. Premier 6.0 software was used to design DEG-specific primers (Additional file 9: Table S4). The real-time fluorescence quantitative PCR system was 20 μL . The two-step method was used for amplification, and the reaction conditions were as follows: predenaturation at 95°C for 30 s, followed by 40 cycles of denaturation at 95°C for 15 s and annealing/extension at 60°C for 30 s. The relative expression levels of each gene were calculated using the $2^{-\Delta\Delta\text{Ct}}$ method [103].

Statistical analysis

SPSS 26.0 statistical software (SPSS Inc., Chicago, IL, USA) was used for statistical analysis, one-way ANOVA and Duncan's test were used to analyze significant differences in physiological parameters, and GraphPad Prism 8.0 software (GraphPad Software, Boston, USA) was used for drawing.

Supplementary Information

The online version contains supplementary material available at <https://doi.org/10.1186/s12870-024-05531-5>.

Supplementary Material 1.
Supplementary Material 2.
Supplementary Material 3.
Supplementary Material 4.
Supplementary Material 5.
Supplementary Material 6.
Supplementary Material 7.
Supplementary Material 8.
Supplementary Material 9.
Supplementary Material 10.
Supplementary Material 11.
Supplementary Material 12.

Acknowledgements

We thank the Gansu Chuanglv Grass Technology Co., Ltd for providing the seeds of *Astragalus cicer* L.

Authors' contributions

Y.Z. performed the experiments, analyzed the data and wrote the manuscript. W.D. conceived the research. W.D., C.Z. and H.M. made helpful comments on our work and manuscript. F.M., Y.W., X.Z., and M.J. provided assistance in data analysis. All authors reviewed the manuscript.

Funding

This study was funded by the Natural Science Foundation of Gansu Provincial Science and Technology Department (22JR5RA871).

Availability of data and materials

Data related to this publication are included in the manuscript and rest of the data is given in supplementary files. Raw Illumina sequence data were deposited in the National Center for Biotechnology Information (NCBI) and be accessed in the sequence read archive (SRA) database (<https://www.ncbi.nlm.nih.gov/sra>). The accession number is PRJNA1079516 (<https://submit.ncbi.nlm.nih.gov/subs/biosample/SUB14268788/overview>).

Declarations

Ethics approval and consent to participate

Experimental research and field studies on plants including the collection of plant material are comply with relevant guidelines and regulation.

Consent for publication

Not applicable.

Competing interests

The authors declare no competing interests.

Received: 19 March 2024 Accepted: 21 August 2024

Published online: 30 August 2024

References

- Zhao Y, Jia KH, Tian YT, Han KJ, El-Kassaby YA, Yang H, Si HY, Sun YH, Li Y. Time-course transcriptomics analysis reveals key responses of populus to salt stress. *Industrial Crops Products*. 2023;194: 116278.
- Brinker M, Brosché M, Vinocur B, Abo-Ogiala A, Fayyaz P, Janz D, Ottow EA, Cullmann AD, Saborowski J, Kangasjärvi J, Altman A, Polle A. Linking the salt transcriptome with physiological responses of a salt-resistant *Populus* species as a strategy to identify genes important for stress acclimation. *Plant Physiol*. 2010;154(4):1697–709.
- Shen W, Gómez-Cadenas A, Routly EL, David Ho TH, Simmonds JA, Gulick PJ. The salt stress-inducible protein kinase gene, *Esi47*, from the salt-tolerant wheat grass *Lophopyrum elongatum* is involved in plant hormone signaling. *Plant Physiol*. 2001;125(3):1429–41.
- Dos Santos TB, Ribas AF, De Souza SGH, Budzinski IGF, Domingues DS. Physiological responses to drought, salinity, and heat stress in plants: A review. *Stresses*. 2022;2(1):113–35.
- Zelm EV, Zhang YX, Testerink C. Salt tolerance mechanisms of plants. *Annu Rev Plant Biol*. 2020;29(71):403–33.
- Zhou HP, Shi HF, Yang YQ, Feng XX, Chen X, Xiao F, Lin HH, Guo Y. Insights into plant salt stress signaling and tolerance. *J Genet Genomics*. 2024;51(1):16–34.
- Zhu JK. Regulation of ion homeostasis under salt stress. *Curr Opin Plant Biol*. 2003;6(5):441–5.
- Lindberg S, Premkumar A. Ion changes and signaling under salt stress in wheat and other important crops. *Plants (Basel)*. 2023;13(1):46.
- Ashraf MA, Shahzad SM, Imtiaz M, Rizwan M, Arif MS, Kausar R. Nitrogen nutrition and adaptation of glycophytes to saline environment: a review. *Archives of Agronomy and Soil Science*. 2018;64:1181–206.
- Ding MQ, Hou PC, Shen X, Wang MJ, Deng SR, Sun J, Xiao F, Wang RG, Zhou XY, Lu CF, Zhang DQ, Zheng XJ, Hu ZM, Chen SL. Salt-induced expression of genes related to Na⁺/K⁺ and ROS homeostasis in leaves of salt-resistant and salt-sensitive poplar species. *Plant Mol Biol*. 2010;73(3):251–69.
- Janz D, Behnke K, Schnitzler JP, Kanawati B, Schmitt-Kopplin P, Polle A. Pathway analysis of the transcriptome and metabolome of salt sensitive and tolerant poplar species reveals evolutionary adaption of stress tolerance mechanisms. *BMC Plant Biol*. 2010;17(10):150.
- Wang T, Tohge T, Ivakov A, Mueller-Roeber B, Fernie AR, Mutwil M, Schippers JHM, Persson S. Salt-related MYB1 coordinates abscisic acid biosynthesis and signaling during salt stress in *Arabidopsis*. *Plant Physiol*. 2015;169(2):1027–41.
- Zhang XY, Tang LH, Nie JW, Zhang CR, Han X, Li QY, Qin L, Wang MH, Huang X, Yu F, Su M, Wang Y, Xu RM, Guo Y, Xie Q, Chen YH. Structure and activation mechanism of the rice salt overly sensitive 1 (*SOS1*) Na⁺/H⁺ antiporter. *Nat Plants*. 2023;9(11):1924–36.
- Tao LY, Wang B, Xin SC, Li W, Huang SC, Liu LH, Cui J, Zhang QR, Cheng XG. A cluster of mutagenesis revealed an osmotic regulatory role of the *OsPIP1* genes in enhancing rice salt tolerance. *The Crop Journal*. 2023;11(4):1204–17.
- Yu ZP, Duan XB, Luo L, Dai SJ, Ding ZJ, Xia GM. How plant hormones mediate salt stress responses. *Trends Plant Sci*. 2020;25(11):1117–30.
- Mac Taggart DR, Billiget B, Lardner HA. Assessment of diverse cicer milkvetch (*Astragalus cicer* L.) germplasm for agro-morphological traits under a stockpiling system. *Can J Plant Sci*. 2023;103(4):389–400.
- Acharya NS, Kastelic PJ, Beauchemin AK, Messenger DF. A review of research progress on cicer milkvetch (*Astragalus cicer* L.). *Can J Plant Sci*. 2006;86(1):49–62.
- Li JC, Tian ZX, Han AH, Li JK, Luo AD, Liu RQ, Zhang ZY. Integrative physiological, critical plant endogenous hormones, and transcriptomic analyses reveal the difenoconazole stress response mechanism in wheat (*Triticum aestivum* L.). *Pestic Biochem Physiol*. 2023;197:105688.
- Zhang B, Horvath S. A general framework for weighted gene co-expression network analysis. *Stat Appl Genet Mol Biol*. 2005;4:Article17.
- Liu HH, Wu HF, Wang Y, Wang H, Chen SH, Yin ZT. Comparative transcriptome profiling and co-expression network analysis uncover the key genes associated with early-stage resistance to *Aspergillus flavus* in maize. *BMC Plant Biol*. 2021;21(1):216.
- Li R, Yang Y, Cao HP, Peng X, Yu Q, He LS, Chen J, Xiang LE, Liu WH. Heterologous expression of the tobacco metallothionein gene *NtMT2F* confers enhanced tolerance to Cd stress in *Escherichia coli* and *Arabidopsis thaliana*. *Plant Physiol Biochem*. 2023;195:247–55.
- Huang SB, Van Aken OV, Schwarzländer M, Belt K, Millar AH. The roles of mitochondrial reactive oxygen species in cellular signaling and stress response in plants. *Plant Physiol*. 2016;171(3):1551–9.
- Wang FB, Liu JC, Zhou LJ, Gang Pan a, Li ZW, Zaidi SHR, Cheng FM. Senescence-specific change in ROS scavenging enzyme activities and regulation of various SOD isozymes to ROS levels in psf mutant rice leaves. *Plant Physiol Biochem*. 2016;109:248–261.
- Zhang G, Wang YH, Wu K, Zhang Q, Feng YN, Miao Y, Yan ZM. Exogenous application of chitosan alleviate salinity stress in Lettuce (*Lactuca sativa* L.). *Hortic*. 2021;7(10):342.
- Zhang XL, Gong XQ, Yu HX, Su XJ, Cheng SY, Huang JW, Lei ZL, Li MJ, Ma FW. The proline-rich protein MdPRP6 confers tolerance to salt stress in transgenic apple (*Malus domestica*). *Sci Hortic*. 2023;308:111581.
- Yuan F, Liang X, Li Y, Yin SS, Wang BS. Methyl jasmonate improves tolerance to high salt stress in the recretohalophyte *Limonium bicolor*. *Funct Plant Biol*. 2018;46(1):82–92.
- Apse MP, Sottosanto JB, Blumwald E. Vacuolar cation/H⁺ exchange, ion homeostasis, and leaf development are altered in a T-DNA insertional mutant of *AtNHX1*, the *Arabidopsis* vacuolar Na⁺/H⁺ antiporter. *Plant J*. 2003;36:229–39.
- Hu LX, Zhang PP, Jiang Y, Fu JM. Metabolomic analysis revealed differential adaptation to salinity and alkalinity stress in kentucky bluegrass (*Poa pratensis*). *Plant Mol Biol Report*. 2015;33:56–68.
- Hameed A, Ahmed MZ, Hussain T, Aziz I, Ahmad N, Gul B, Nielsen BL. Effects of salinity stress on chloroplast structure and function. *Cells*. 2021;10(8):2023.
- Miller G, Suzuki N, Ciftci-Yilmaz S, Mittler R. Reactive oxygen species homeostasis and signaling during drought and salinity stresses. *Plant, Cell Environ*. 2010;33:453–67.
- Yang YQ, Guo Y. Elucidating the molecular mechanisms mediating plant salt-stress responses. *New Phytol*. 2018;217(2):523–39.
- Gao Y, Dong X, Wang RG, Hao F, Zhang H, Zhang YY, Lin GL. Exogenous calcium alleviates oxidative stress caused by salt stress in peanut seedling roots by regulating the antioxidant enzyme system and flavonoid biosynthesis. *Antioxidants*. 2024;13(2):233.
- Müller B, Sheen J. *Arabidopsis* cytokinin signaling pathway. *Sci STKE*. 2007;407:cm5.
- Bhattacharjee O, Raul B, Ghosh A, Bhardwaj A, Bandyopadhyay K, Sinharoy S. Nodule INception-independent epidermal events lead

- to bacterial entry during nodule development in peanut (*Arachis hypogaea*). *New Phytol.* 2022;236(6):2265–81.
35. He Q, Yuan RR, Zhang TT, An FY, Wang N, Lan JQ, Wang XIX, Zhang ZL, Pan YG, Wang XZ, Zhang JZ, Guo DS, Qin GJ. *Arabidopsis TIE1* and *TIE2* transcriptional repressors dampen cytokinin response during root development. *Sci Adv.* 2022;8(36):eabn5057.
 36. Yin P, Liang XY, Zhao HS, Xu ZP, Chen LM, Yang XH, Qin F, Zhang JB, Jiang CF. Cytokinin signaling promotes salt tolerance by modulating shoot chloride exclusion in maize. *Mol Plant.* 2023;16(6):1031–47.
 37. To JP, Kieber JJ. Cytokinin signaling: two-components and more. *Trends Plant Sci.* 2008;13(2):85–92.
 38. Mason MG, Jha D, Salt DE, Tester M, Hill K, Kieber JJ, Schaller GE. Type-B response regulators *ARR1* and *ARR12* regulate expression of *ATHKT1;1* and accumulation of sodium in *Arabidopsis* shoots. *Plant J.* 2010;64(5):753–63.
 39. To JPC, Haberer G, Ferreira FJ, Derue' re J, Mason MG, Schaller GE, Alonso GE, Ecker JR, Kieber JJ. Type-A *Arabidopsis* response regulators are partially redundant negative regulators of cytokinin signaling. *Plant Cell.* 2004;16:658–71.
 40. Argyros RD, Mathews DE, Chiang YH, Palmer CM, Thibault DM, Etheridge N, Argyros DA, Mason MG, Kieber JJ, Schaller GE. Type B response regulators of *Arabidopsis* play key roles in cytokinin signaling and plant development. *Plant Cell.* 2008;20(8):2102–16.
 41. Nguyen KH, Ha CV, Nishiyama R, Watanabe Y, Leyva-González MA, Fujita Y, Tran UT, Li W, Tanaka M, Seki M, Schaller GE, Herrera-Estrella L, Tran LS. *Arabidopsis* type B cytokinin response regulators *ARR1*, *ARR10*, and *ARR12* negatively regulate plant responses to drought. *Proc Natl Acad Sci USA.* 2016;113(11):3090–5.
 42. Kim CY, Liu Y, Thorne ET, Yang HP, Fukushige H, Gassmann W, Hildebrand D, Sharp RE, Zhang SQ. Activation of a stress-responsive mitogen-activated protein kinase cascade induces the biosynthesis of ethylene in plants. *Plant Cell.* 2003;15(11):2707–18.
 43. Bleecker AB, Kende H. Ethylene: a gaseous signal molecule in plants. *Annu Rev Cell Dev Biol.* 2000;16:1–18.
 44. Cao WH, Liu J, He XJ, Mu RL, Zhou HL, Chen SY, Zhang JS. Modulation of ethylene responses affects plant salt-stress responses. *Plant Physiol.* 2007;143(2):707–19.
 45. Potuschak T, Lechner E, Parmentier Y, Yanagisawa S, Grava S, Koncz C, Genschik P. EIN3-dependent regulation of plant ethylene hormone signaling by two *Arabidopsis* F box proteins: EBF1 and EBF2. *Cell.* 2003;115(6):679–89.
 46. Jain M, Nijhawan A, Arora R, Agarwal P, Ray S, Sharma P, Kapoor S, Tyagi AK, Khurana JP. F-box proteins in rice. Genome-wide analysis, classification, temporal and spatial gene expression during panicle and seed development, and regulation by light and abiotic stress. *Plant Physiol.* 2007;143(4):1467–83.
 47. Guo XK, Zhang Y, Tu Y, Wang YZ, Cheng WJ, Yang YW. Overexpression of an EIN3-binding F-box protein2-like gene caused elongated fruit shape and delayed fruit development and ripening in tomato. *Plant Sci.* 2018;272:131–41.
 48. De Boer K, Tillemans S, Pauwels L, Vanden Bossche R, De Sutter V, Vanderhaeghen R, Hilson P, Hamill JD, Goossens A. APETALA2/ETHYLENE RESPONSE FACTOR and basic helix-loop-helix tobacco transcription factors cooperatively mediate jasmonate-elicited nicotine biosynthesis. *Plant J.* 2011;66(6):1053–65.
 49. Taketa S, Amano S, Tsujino Y, Sato T, Saisho D, Kakeda K, Nomura M, Suzuki T, Matsumoto T, Sato K, Kanamori H, Kawasaki S, Takeda K. Barley grain with adhering hulls is controlled by an *ERF* family transcription factor gene regulating a lipid biosynthesis pathway. *Proc Natl Acad Sci USA.* 2008;105(10):4062–7.
 50. Zhang GY, Chen M, Li LC, Xu ZS, Chen XP, Guo JM, Ma YZ. Overexpression of the soybean *GmERF3* gene, an AP2/ERF type transcription factor for increased tolerances to salt, drought, and diseases in transgenic tobacco. *J Exp Bot.* 2009;60(13):3781–96.
 51. Siddikee MA, Chauhan PS, Anandham R, Han GH, Sa T. Isolation, characterization, and use for plant growth promotion under salt stress, of *ACC* deaminase-producing halotolerant bacteria derived from coastal soil. *J Microbiol Biotechnol.* 2010;20(11):1577–84.
 52. Rodriguez MC, Petersen M, Mundy J. Mitogen-activated protein kinase signaling in plants. *Annu Rev Plant Biol.* 2010;61:621–49.
 53. Chang Y, Yang HL, Ren DT, Li Y. Activation of ZmMCK10, a maize mitogen-activated protein kinase kinase, induces ethylene-dependent cell death. *Plant Sci.* 2017;264:129–37.
 54. Teige M, Scheikl E, Eulgem T, Dóczi R, Ichimura K, Shinozaki K, Dangl JL, Hirt H. The *MKK2* pathway mediates cold and salt stress signaling in *Arabidopsis*. *Mol Cell.* 2004;15(1):141–52.
 55. Hwa CM, Yang XC. The *AtMCK3* pathway mediates ABA and salt signaling in *Arabidopsis*. *Acta Physiol Plant.* 2008;30(3):277–86.
 56. Xiong LZ, Yang YN. Disease resistance and abiotic stress tolerance in rice are inversely modulated by an abscisic acid-inducible mitogen-activated protein kinase. *Plant Cell.* 2003;15(3):745–59.
 57. Shakeel SN, Wang X, Binder BM, Schaller GE. Mechanisms of signal transduction by ethylene: overlapping and non-overlapping signalling roles in a receptor family. *Arabidopsis.* 2013;5:pl010.
 58. Bishopp A, Mähönen AP, Helariutta Y. Signs of change: hormone receptors that regulate plant development. *Development.* 2006;133(10):1857–69.
 59. Subbiah V, Reddy KJ. Interactions between ethylene, abscisic acid and cytokinin during germination and seedling establishment in *Arabidopsis*. *J Biosci.* 2010;35(3):451–8.
 60. Wilson RL, Kim H, Bakshi A, Binder BM. The ethylene receptors ETHYLENE RESPONSE1 and ETHYLENE RESPONSE2 have contrasting roles in seed germination of *Arabidopsis* during salt stress. *Plant Physiol.* 2014;165(3):1353–66.
 61. Feng L, Teng F, Li N, Zhang JC, Zhang BJ, Tsai SN, Yue XL, Gu LF, Meng GH, Deng TQ, Tong SW, Wang CM, Li Y, Shi W, Zeng YL, Jiang YM, Yu WC, Ngai SM, An LZ, Lam HM, He JX. A reference-grade genome of the xerophyte *Ammopiptanthus mongolicus* sheds light on its evolution history in legumes and drought-tolerance mechanisms. *Plant Commun.* 2024;5(7):100891.
 62. Meng FY, Feng NJ, Zheng DIF, Liu ML, Zhang RJ, Huang XX, Huang AQ, Chen ZM. Exogenous hemin alleviates NaCl stress by promoting photosynthesis and carbon metabolism in rice seedlings. *Sci Rep.* 2023;13(1):3497.
 63. Hao SH, Wang YR, Yan YX, Liu YH, Wang JY, Chen S. A review on plant responses to salt stress and their mechanisms of salt resistance. *Horticulturae.* 2021;7(6):132.
 64. Shu S, Guo SR, Sun J, Yuan LY. Effects of salt stress on the structure and function of the photosynthetic apparatus in *Cucumis sativus* and its protection by exogenous putrescine. *Physiol Plant.* 2012;146(3):285–96.
 65. López-Calcagno PE, Brown KL, Simkin AJ, Fisk SJ, Viallet-Chabrand S, Lawson T, Raines CA. Stimulating photosynthetic processes increases productivity and water-use efficiency in the field. *Nat Plants.* 2020;6(8):1054–63.
 66. Chen JH, Tang M, Jin XQ, Li H, Chen LS, Wang QL, Sun AZ, Yi Y, Guo FQ. Regulation of Calvin-Benson cycle enzymes under high temperature stress. *Abiotech.* 2022;3(1):65–77.
 67. Lu L, Wu XR, Tang Y, Zhu LM, Hao ZD, Zhang JB, Li XL, Shi JS, Chen JH, Cheng TL. Halophyte *Nitraria billardieri CIPK25* promotes photosynthesis in *Arabidopsis* under salt stress. *Front Plant Sci.* 2022;13:1052463.
 68. Meloni M, Gurrieri L, Fermani S, Velie L, Sparla F, Crozet P, Henri J, Zaffagnini M. Ribulose-1,5-bisphosphate regeneration in the Calvin-Benson-Bassham cycle: Focus on the last three enzymatic steps that allow the formation of Rubisco substrate. *Front Plant Sci.* 2023;14:1130430.
 69. Li Y, Liu ZL, Shi QH, Yang FJ, Wei M. Mixed red and blue light promotes tomato seedlings growth by influencing leaf anatomy, photosynthesis, CO₂ assimilation and endogenous hormones. *Sci Hortic.* 2021;290:110500.
 70. Millar AH, Whelan J, Soole KL, Day DA. Organization and regulation of mitochondrial respiration in plants. *Annu Rev Plant Biol.* 2011;62(1):79–104.
 71. Le XH, Lee CP, Millar AH. The mitochondrial pyruvate carrier (MPC) complex mediates one of three pyruvate-supplying pathways that sustain *Arabidopsis* respiratory metabolism. *Plant Cell.* 2021;33(8):2776–93.
 72. Simkin AJ, Alqurashi M, Lopez-Calcagno PE, Headland LR, Raines CA. Glyceraldehyde-3-phosphate dehydrogenase subunits A and B are essential to maintain photosynthetic efficiency. *Plant Physiol.* 2023;192(4):2989–3000.
 73. Anoman AD, Muñoz-Bertomeu J, Rosa-Téllez S, Flores-Tornero M, Serrano R, Bueso E, Fernie AR, Segura J, Ros R. Plastidial glycolytic glyceraldehyde-3-phosphate dehydrogenase is an important

- determinant in the carbon and nitrogen metabolism of heterotrophic cells in *Arabidopsis*. *Plant Physiol.* 2015;169:1619–37.
74. Anderson LE, Bryant JA, Carol AA. Both chloroplastic and cytosolic phosphoglycerate kinase isozymes are present in the pea leaf nucleus. *Protoplasma.* 2004;223(2–4):103–10.
 75. Rosa-Téllez S, Anoman AD, Flores-Tornero M, Toujani W, Alseek S, Fernie AR, Nebauer SG, Muñoz-Bertomeu J, Segura J, Ros R. Phosphoglycerate kinases are Co-regulated to adjust metabolism and to optimize Growth. *Plant Physiol.* 2018;176(2):1182–98.
 76. Wu Y, Liu HM, Bing J, Zhang GF. Integrative transcriptomic and TMT-based proteomic analysis reveals the mechanism by which *AtENO2* affects seed germination under salt stress. *Front Plant Sci.* 2022;13:1035750.
 77. Wang QJ, Sun H, Dong QL, Sun TY, Jin ZX, Hao YJ, Yao YX. The enhancement of tolerance to salt and cold stresses by modifying the redox state and salicylic acid content via the cytosolic malate dehydrogenase gene in transgenic apple plants. *Plant Biotechnol J.* 2016;14(10):1986–97.
 78. Condori-Apfata JA, Batista-Silva W, Medeiros DB, Vargas JR, Valente LML, Pérez-Díaz JL, Fernie AR, Araújo WL, Nunes-Nesi A. Downregulation of the E2 subunit of 2-oxoglutarate dehydrogenase modulates plant growth by impacting Carbon-Nitrogen metabolism in *Arabidopsis thaliana*. *Plant Cell Physiol.* 2021;62(5):798–814.
 79. Araújo WL, Nunes-Nesi A, Trenkamp S, Bunik VI, Fernie AR. Inhibition of 2-oxoglutarate dehydrogenase in potato tuber suggests the enzyme is limiting for respiration and confirms its importance in nitrogen assimilation. *Plant Physiol.* 2008;148(4):1782–96.
 80. Benidickson KH, Raytek LM, Hoover GJ, Flaherty EJ, Shelp BJ, Snedden WA, Plaxton WC. Glutamate decarboxylase-1 is essential for efficient acclimation of *Arabidopsis thaliana* to nutritional phosphorus deprivation. *New Phytol.* 2023;240(6):2372–85.
 81. Joshi J, Folz JS, Gregory JF III, McCarty DR, Fiehn O, Hanson AD. Rethinking the *PDH* bypass and *GABA* shunt as thiamin-deficiency workarounds. *Plant Physiol.* 2019;181:389–93.
 82. Shen BR, Wang LM, Lin XL, Yao Z, Xu HW, Zhu CH, Teng HY, Cui LL, Liu EE, Zhang JJ, He ZH, Peng XX. Engineering a new chloroplastic photorespiratory bypass to increase photosynthetic efficiency and productivity in rice. *Mol Plant.* 2018;12(2):199–214.
 83. Roell MS, Schada von Borzykowski L, Westhoff P, Plett A, Paczia N, Claus P, Urte S, Erb TJ, Weber APM. A synthetic C4 shuttle via the β -hydroxyaspartate cycle in C3 plants. *Natl Acad Sci.* 2021;118(21):e2022307118.
 84. Schmitz J, Hüdig M, Meier D, Linka N, Maurino VG. The genome of *Ricinus communis* encodes a single glycolate oxidase with different functions in photosynthetic and heterotrophic organs. *Planta.* 2020;252(6):100.
 85. Betti M, Bauwe H, Busch FA, Fernie AR, Keech O, Levey M, Ort DR, Parry MA, Sage R, Timm S, Walker B, Weber AP. Manipulating photorespiration to increase plant productivity: recent advances and perspectives for crop improvement. *J Exp Bot.* 2016;67(10):2977–88.
 86. Hoshida H, Tanaka Y, Hibino T, Hayashi Y, Tanaka A, Takabe T. Enhanced tolerance to salt stress in transgenic rice that overexpresses chloroplast glutamine synthetase. *Plant Mol Biol.* 2000;43:103–11.
 87. Sami F, Yusuf M, Faizan M, Faraz A, Hayat S. Role of sugars under abiotic stress. *Plant Physiol Biochem.* 2016;109:54–61.
 88. Price J, Laxmi A, Martin SK, Jang JC. Global transcription profiling reveals multiple sugar signal transduction mechanisms in *Arabidopsis*. *Plant Cell.* 2004;16:2128–50.
 89. Gibson SI. Sugar and phytohormone response pathways: navigating a signalling network. *J Experiment Bot.* 2004;55(395):253–64.
 90. Xing X, Liu YK, Kong XP, Liu Y, Li DQ. Overexpression of a maize dehydrin gene, *ZmDHN2b*, in tobacco enhances tolerance to low temperature. *Plant Growth Regul.* 2011;65(1):109–18.
 91. Heath RL, Packer L. Photoperoxidation in isolated chloroplasts: I. Kinetics and stoichiometry of fatty acid peroxidation. *Arch Biochem Biophys.* 1968;125(1):189–98.
 92. Bates LS, Waldren RP, Teare ID. Rapid determination of free proline for water-stress studies. *Plant Soil.* 1973;39(1):205–7.
 93. Yemm EW, Willis AJ. The estimation of carbohydrates in plant extracts by anthrone. *Biochem J.* 1954;57(3):508–14.
 94. Jia CH, Yu XJ, Zhang M, Liu ZG, Zou P, Ma J, Xu YC. Application of melatonin-enhanced tolerance to high-temperature stress in cherry radish (*Raphanus sativus* L. var. *radculus pers*). *J Plant Growth Reg.* 2019;39(2):1–10.
 95. Giannopolitis CN, Ries SK. Superoide dismutase: Occurrence in higher plants. *Plant Physiol.* 1997;59(2):309–13.
 96. Fu J, Huang B. Involvement of antioxidants and lipid peroxidation in the adaptation of two cool-season grasses to localized drought stress. *Environ Exp Bot.* 2001;45(2):105–14.
 97. Singh S, Singh M. Genotypic basis of response to salinity stress in some crosses of spring wheat *Triticum aestivum* L. *Euphytica.* 2000;115(3):209–14.
 98. Elstner EF, Heupel A. Inhibition of nitrite formation from hydroxylammonium chloride: a simple assay for superoxide dismutase. *AnalBiochem.* 1976;70:616–20.
 99. Becana M, Aparicio-Tejo P, Irigoyen JJ, Sanchez-Diaz M. Some enzymes of hydrogen peroxide metabolism in leaves and root nodules of *Medicago sativa*. *Plant Physiol.* 1986;82(4):1169–71.
 100. Chen T, Liu YX, Huan LQ. ImageGP: An easy-to-use data visualization web server for scientific researchers. *Imeta.* 2022;1(1):e5.
 101. Ren Y, Yu G, Shi CP, Liu LM, Guo Q, Han C, Zhang D, Zhang L, Liu BX, Gao H, et al. Majorbio Cloud: A one-stop, comprehensive bioinformatic platform for multi-omics analyses. *IMeta.* 2022;1(2):e12.
 102. Dong WK, Ma HL, Chen CY, Li YZ. Overexpression of the *OvBAN* gene enhances the proanthocyanidin content in transgenic alfalfa (*Medicago sativa* L.). *In Vitro Cell Dev Biol.* 2020;56(4):548–57.
 103. Livak KJ, Schmittgen TD. Analysis of relative gene expression data using real-time quantitative PCR and the $2^{-\Delta\Delta C(T)}$ Method. *Meth-ods.* 2001;25:402–8.

Publisher's Note

Springer Nature remains neutral with regard to jurisdictional claims in published maps and institutional affiliations.